

AN HISTORICAL REVIEW OF THE HYDRODYNAMIC THEORY OF BOILING

JOHN H. LIENHARD and LARRY C. WITTE

*Heat Transfer/Phase Change Laboratory
Mechanical Engineering Department
University of Houston - University Park
Houston, TX 77004, USA*

CONTENTS

	Page
1. Introduction	189
2. History of the Hydrodynamic Theory Before 1958	190
2.1. Early Observations of the Hydrodynamic Transitions	190
2.2. The Boiling Curve	193
2.3. The Problem of Transition Boiling	196
2.4. Precursors of the Zuber-Tribus Theory	199
2.5. Interfacial Stability Theory Before WWII	202
2.6. Early Post-War Formulations	204
3. The Zuber-Tribus Model	211
3.1. Zuber's Set of Hydrodynamic Transitions	211
3.2. Zuber's Diagnosis of Transition Boiling	212
3.3. Formulation of the q_{\max} Prediction	214
3.4. Formulation of the q_{\min} Prediction	216
3.5. Early Reactions to the Hydrodynamic Theory	217
4. Subsequent Articulations of the Zuber-Tribus Theory	220
4.1. Berenson's Transition Boiling Study	220
4.2. The Zuber-Moissis-Berenson Transition	222
4.3. Film Boiling on a Horizontal Cylinder	224
4.4. Burnout on a Horizontal Cylinder	229
4.5. The Dhir-Lienhard Predictions	233
5. The Hydrodynamic Theory of Flow Boiling	243
5.1. Induced Convection	243
5.2. Burnout During Crossflow over a Horizontal Cylinder	245
5.3. Burnout in the Jet-Disc Configuration	251
6. The Transition Boiling Region Revisited	254
6.1. The View of the Transition Boiling Region in 1980	254

6.2. The Witte-Lienhard Proposal	258
6.3. Recent Findings	260
7. Summary	265
7.1. The State of the Hydrodynamic Theory Today	265
7.2. Some General Observations on Research in this Area	267
8. References	270
9. Nomenclature	278

“Perhaps the most striking feature of...normal research problems...is how little they aim to produce major novelties...”

Thomas S. Kuhn

1. Introduction

Engineers began to recognize the enormous potential of boiling for transferring heat under low temperature differences, during the 1930's. Over twenty years ago Gouse [1] traced the intervening exponential growth in the number of citations in boiling and two-phase flow in a heroic literature survey of over 6000 citations. To duplicate his feat today would sorely try anyone's stamina.

What we call the *Hydrodynamic Theory of Boiling* in this paper has been in the public eye ever since Zuber's Ph.D. dissertation under Tribus in 1958 [2,3]. The dissertation, titled *Hydrodynamic Aspects of Boiling*, was an audacious and far ranging study that awakened passionate and heated opposition. It was a work which, while not correct in all its details, ranks among the small handful of true milestones in this staggering profusion of writings.

To speak of a hydrodynamic theory of boiling will at first seem hopelessly unrestrictive, since every aspect of boiling involves hydrodynamic processes in which vapor leaves a heater while liquid moves in towards it. The name generally refers to the several transitions in boiling behavior that result from hydrodynamic instabilities in the vapor escape processes.

These transitions include the *peak heat flux*, or *burnout* transition, the transition from isolated bubbles to slugs-and-columns action in nucleate boiling, the *minimum heat flux* which may or may not be a true hydrodynamic transition, and one or more transitions in the “transition boiling” regime that are dictated by contact angle behavior. In addition to hydrodynamically dictated transitions, much of the regular vapor escape behavior in boiling is dictated by the cyclic collapse of Taylor-Helmholtz unstable vapor escape structures. The two most notable examples are the Taylor wave “bubble-escapement” pattern in film boiling and the placement of liquid jets near the peak nucleate boiling heat flux.

This body of theory evolved only after observations of the various boiling instability phenomena had become sufficiently well-defined to permit its articulation, and after the postwar extensions of the Taylor-Helmholtz theory had provided the tools for its formulation. Our present aim is to trace the historic antecedents of the theory; to describe its formulation and its early

struggle for survival; to follow its exploitation during the 1960's and 1970's, and to show where the theory presently fails to provide answers to some major questions.

We shall see that Zuber's original formulation of the Hydrodynamic Theory began with the least understood aspect of boiling behavior, namely *transition boiling*; that for years it has been articulated without significant reference to this regime; and that new discoveries about the behavior of transition boiling are only now leading us to re-interpretations of the theory.

2. History of the Hydrodynamic Theory Before 1958

2.1. Early Observations of the Hydrodynamic Transitions

It is significant that the earliest systematic description of boiling quoted in the literature deals with the major hydrodynamic transition that marks the boiling process. In 1756, Leidenfrost /4/ introduced various numbers of drops of water into the bowl of a heavy metal spoon heated to different temperatures. He found that if the spoon were heated only slightly above the normal boiling point of water, the water would bubble away within a second or so. But when the spoon was made red-hot, the water would pull into spherical drops, dance about in the bowl of the spoon, and take upward of a minute to convert to steam.

However, Kistemaker /5/ notes that both Boerhaave (1732) (whom Leidenfrost quotes) and Elder (1746) had studied the phenomenon previously. He attributes the term "spheroidal state" (in reference to the droplets) to Boutigny (1843), and credits Stark (1898) with later studies of the form of the drops. Kutateladze (/6/, Chapter 9) refers to more quantitative 19th century observations by Gezekhus (1876) who plotted the survival time of a standard drop of water, as the surface temperature was varied.

Nukiyama's /7/ quantitative re-creation of Leidenfrost's experiment in 1934 is normally cited as being the first modern consideration of the boiling transitions. Nukiyama devised the experiment, shown in Fig. 1, that did so much to clarify Leidenfrost's observation. He simultaneously used a horizontal wire as a heater, and as a resistance thermometer. This way he simultaneously measured the heat flux, q , and the wall superheat, $T_{\text{wall}} - T_{\text{sat}} \equiv \Delta T$. The result was an enormous hysteresis loop. First the wall superheat increased very little as the heat flux rose to a very high value. Then it suddenly leaped by a thousand or so degrees. After that, the wall superheat stayed quite high while the heat flux was reduced to a very low value. Finally, the wall superheat suddenly dropped back to almost nothing.

Nukiyama not only observed the peak and minimum heat flux limits, he

also speculated that, had he been able to vary the wall superheat independently, he would have been able to measure the connecting dashed line in the figure.

Of course, boiling had not been ignored during the two centuries that separated Nukiyama from Leidenfrost. In his paper, Nukiyama cites previous measurements of the q vs. ΔT relationship in nucleate boiling by Austin (1902), and by Jakob and Linke (1933). These data show the heat flux rising with temperature difference, but they offer no suggestion that the rise might reach a limit.

Furthermore, Nukiyama did not actually present the first boiling curves. Early in this century, metallurgists concerned with the influence of cooling rates on the structure of metals turned to quenching experiments. In 1919, Pilling and Lynch [8] quenched 0.64 cm dia. cylindrical samples with thermocouples embedded in them. Their concern was not with heat transfer, q , but with the cooling rates ($^{\circ}\text{C}/\text{s}$) which are virtually equivalent.

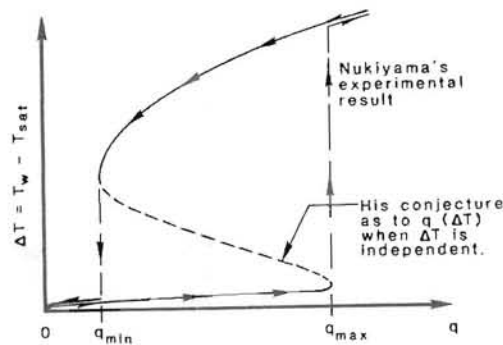
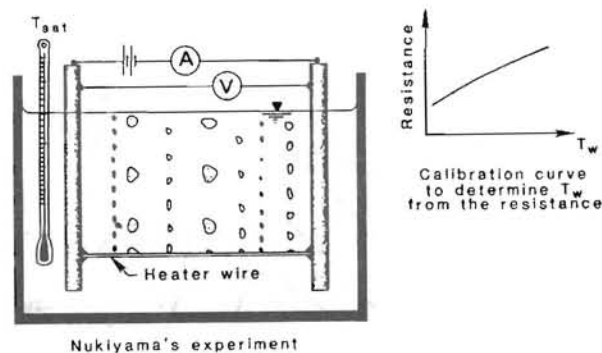


Fig. 1 Nukiyama's experiment and its result.

Figure 2 is a copy of one of their plots of cooling rates as a function of cylinder temperature, for several initial water temperatures. These curves — particularly for quenches in near-saturated water — have the same general form as the boiling curve in Fig. 1, with the coordinates reversed. Pilling and Lynch identify the film boiling region¹ as “Cooling in vapor,” the transition through nucleate region as “Cooling by active vaporization,” and the natural convection region as “Cooling in liquid.”

The presence of the Pilling-Lynch paper dramatizes a dilemma that faces any historian of science or technology when he tries to discuss *priority*. We are tempted to claim that they do not deserve credit for discovering the multivalued character of the boiling curve because they did not explicitly address heat transfer. We feel we must speak of this behavior in terms of heat flux, and their work seems out of context. Yet it is clear that, had Nukiyama known of these data, he would have been obliged to write about his own

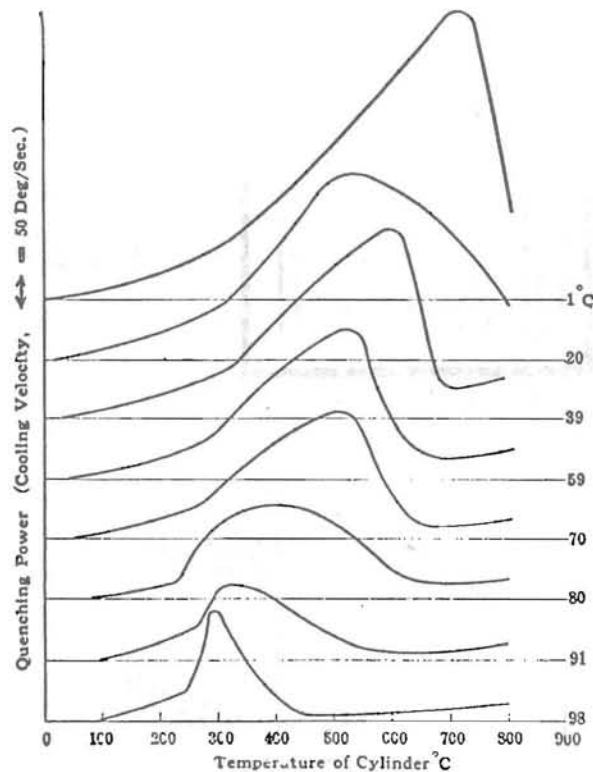


Fig. 2 One of Pilling's and Lynch's sets of quenching curves.

¹ These boiling regimes are explained more fully below.

experiments in vastly different terms. Indeed, our understanding of things would almost certainly have been hastened, had Nukiyama known of the Pilling-Lynch work or, for that matter, even the earlier Gezekhus experiments.

This may seem a philosophical point, but it will return again and again to haunt us, even in this paper. Any very clever interpretation of nature inevitably has precursors that have failed to claim people's attention. The person who eventually stands to receive credit for inventing a new "scientific" description is the one who manages to present it in such a way as to cause the current practitioners' view to shift discontinuously.

Three years after Nukiyama's work Drew and Mueller /9/ did a fairly qualitative little experiment in which they approximated a controlled surface-temperature situation. Their strategy involved heating a copper tube from within, with condensing steam, and boiling a more volatile liquid outside. They were thus able to fill in a few points which suggested that Nukiyama's conjectured dotted line actually existed.

2.2. The Boiling Curve

Figure 3 is a reasonable scale representation of the actual boiling curve that one might actually get in a well-executed modern experiment, using boiling water at atmospheric pressure on a large, clean, smooth, not-too-well-wetted, flat plate. These curves are frequently drawn horribly out-of-scale in heat transfer books. Authors who have not worked in boiling have a hard time believing how great the hysteresis effect can sometimes be.

We identify five regions in this curve: All but the first are illustrated photographically in Fig. 4. (Figures 1 and 2 are taken from /10/. Figures 3 and 4 have been adapted from /10/.)

- The first region is that of *natural convection*, in which the slightly-superheated, single-phase liquid buoys off the heater.
- There are two distinct nucleate boiling regimes: the region of *isolated bubbles* at lower heat fluxes...
- ...and the region of *slugs and columns* at higher heat fluxes. The region of slugs and columns ends at the *peak* or *burnout* heat flux, q_{\max} .
- The region in which the heat flux decreases with wall superheat, is the *transition boiling* region. It cannot be reached when q is varied independently. We represent the transition boiling curve as both dashed and broken for reasons that will be explained later. (These photos were taken by the first author in a re-creation of the Drew-Mueller experiment.)
- The leg on the right is called the *film boiling* regime, which may or may not end at the *minimum heat flux*, q_{\min} .

Our failure to represent transition boiling with a definite continuous line; our refusal to identify all points above q_{\min} on the right as film boiling; and our suggestion that Drew and Mueller's experiments might not actually represent a true independent specification of ΔT — all of these matters represent changes in thinking about the boiling curve that arose many decades later. But, at the time, Drew and Mueller's crude experiment had firmly established a picture of the boiling curve in people's minds.

Kuhn's [11] essay on the nature of scientific revolutions does much to explain what occurred subsequently. (In fact, the preceding arguments about the nature of scientific priority also originate with Kuhn.) Kuhn argued

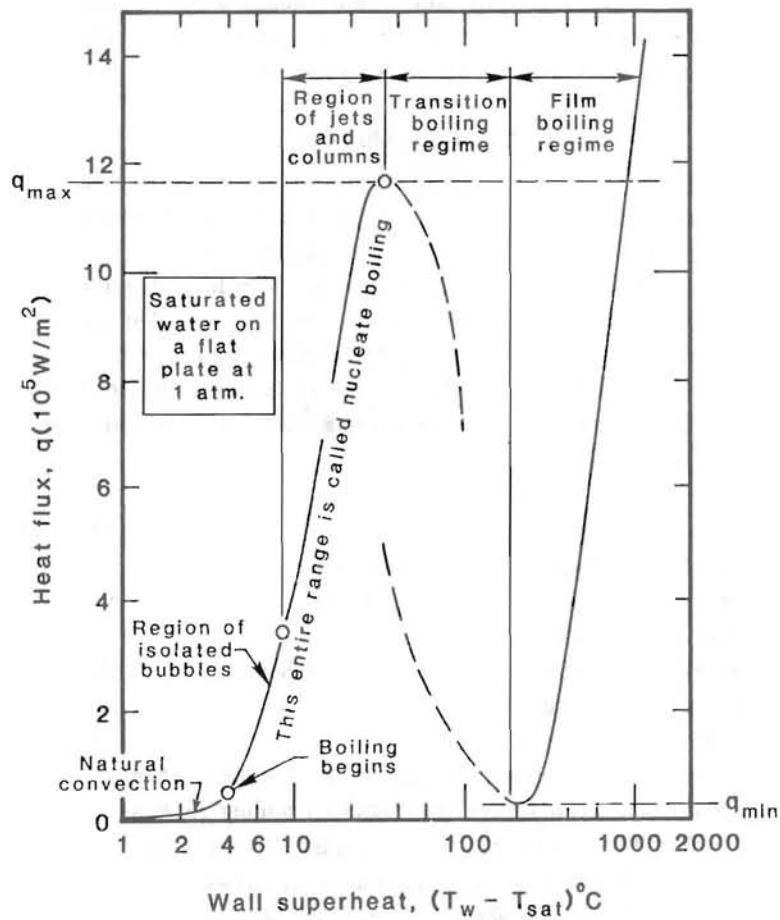
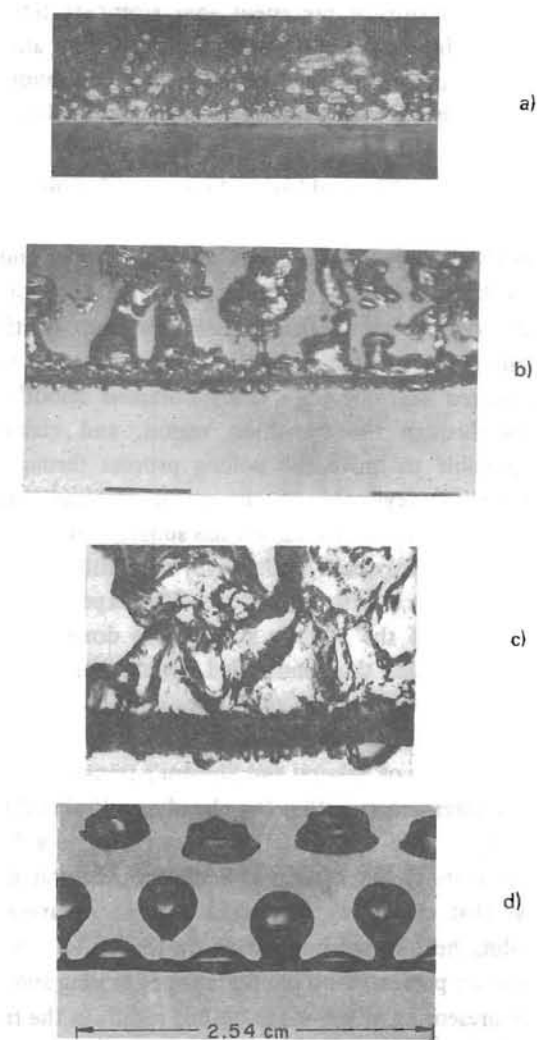


Fig. 3 Typical boiling curve and regimes of boiling for an unspecified heater.



a) Isolated bubble region (water)

b) 0.322 mm dia. wire in methanol at 10 earth-normal gravities, $q = 0.35 \text{ MW/m}^2$

c) "Nucleate-transition" boiling of acetone on a 3.2. mm dia. tube

d) Film boiling of acetone on a 0.646 mm dia. wire near q_{\min}

Fig. 4 Typical photographs of boiling in the regimes identified in Fig. 3.

convincingly from historical precedent that scientists repeatedly see what they expect to see in experiments. Nukiyama, and Drew and Mueller, told us that the transition boiling regime should form a continuous curve between q_{\max} to q_{\min} and that is what subsequent investigators found.

2.3. The Problem of Transition Boiling

We believe the famous boiling curves given by Farber and Scoriah /12/ in 1948 illustrate Kuhn's claim. They offers q vs. ΔT data for pool boiling on small wires at various pressures, using electric resistance heating which — they conceded — should be very unstable. The temperature was measured with an *externally mounted* thermocouple. They obtained smooth and continuous boiling curves through the transition region, and claimed that it was "frequently possible to move the boiling process through the conditions [along the transition regime]" by the artful manipulation of the electric supply — something that no investigator has subsequently been able to do.

As late as 1974, Sakurai and Shiotsu /13/ were still trying to penetrate the transition boiling regime with a q -independent experiment. However, their artful manipulation of the electric supply was done with a sophisticated feedback control system that controlled the temperature of the wire — a system first developed by Peterson and Zaalouk /14/ — and their temperatures were obtained by measuring the resistance of the wire.

The startling feature of Sakurai and Shiotsu's transition boiling data is that they form a hysteresis loop within the already multiple-valued boiling curve, as shown in Fig. 5. The upper of these two curves is a form of transition boiling that we identify and discuss in Section 6. Sakurai and Shiotsu's text made it clear that the lower curve was a locus of averages of film and transition boiling heat fluxes co-existing on the heater. By the same token, Farber and Scoriah presented no photographs of boiling and it is possible that they too were presenting mixed-mode boiling results in the transition regime.

In 1983, Zhukov and Barelko /15/ supported these suspicions when they concluded that the "usual technical means of controlling the temperature regime of a heat generating element are insufficient to provide reliable information on the true boiling curve in the transitional region." Only through very sophisticated electrical control systems were they able to measure what they consider the true values of the burnout and minimum heat fluxes on thin wires. And even then, they could not trace out the entire transition boiling regime.

Even systems heated by condensing vapors cannot generally trace out the entire transition regime; yet Drew's and Mueller's inference led many

investigators to draw continuous lines connecting points, measured in the transition regime, to the burnout and minimum heat flux points. This was common practice through the 1950's, 1960's, and into the 1970's. In 1956, Pramuk and Westwater /16/ obtained the data shown in Fig. 6. The uncertainty of those points in the transition regime was fairly high — on the order of ± 20 percent. We include the line they drew through these data, with the portion that we distrust (on the basis of 30 years of hindsight) shown as a dashed line.

Four years later, Berenson /17/ made the most carefully contrived measurements of transition boiling up to that time. He boiled several organic fluids on a thick horizontal copper plate heated by water condensing under pressure on the finned bottom side. He carefully noted the effect of varying the finish and surface chemistry of the upper boiling plate.

Berenson's system for regulating ΔT had an important weakness that was recognized a few years later by Stefan and Kovalev, and Grassman and Ziegler (see e.g. Hesse /18/) who pointed out that in such systems

$$q = (T_{\text{cond. stm.}} - T_{\text{sat}}) / \Sigma R_t = (T_w - T_{\text{sat}}) / R_b \tag{1}$$

where R_b is the thermal resistance of the boiling process and ΣR_t is the sum of the thermal resistances between the condensing steam and the saturated boiled liquid. The rearrangement of the two equations (1) gives

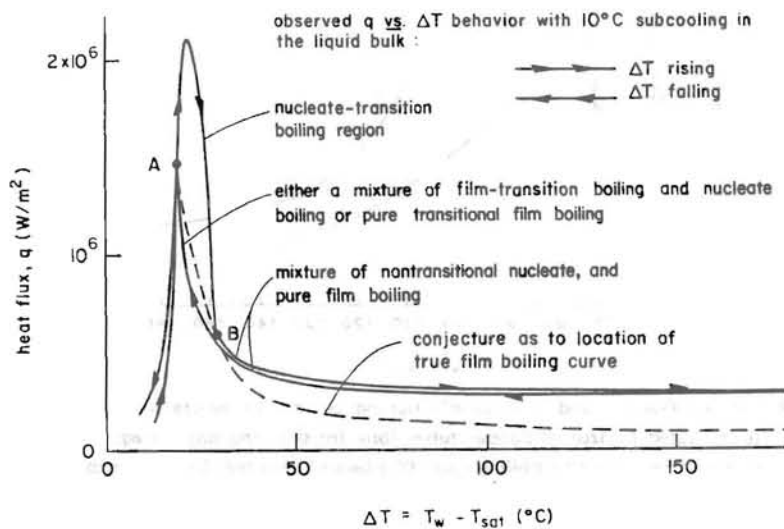


Fig. 5 Sakurai and Shiotsu's "transition boiling" data.

$$\Delta T = (T_{\text{cond. stm.}} - T_{\text{sat}}) - (\Sigma R_t - R_b)q \quad (2)$$

In other words, the system can only reach those $(q, \Delta T)$ pairs on q vs. ΔT coordinates that lie on lines passing through ΔT on the abscissa with a negative slope equal to the inverse thermal resistance of all elements between the condensing steam and the boiling surface. (We return to this matter in Section 6.1.)

Figure 7 shows a typical set of Berenson's data. We have removed a continuous (and, we believe, misleading) line which he had originally drawn through the data. Slanting "access lines" given by equation (2) are overlaid on the curve. These are based on Berenson's copper block resistance ($0.0001514 \text{ m}^2\text{-}^\circ\text{C/W}$) and, since the bottom side was finned, zero condensing resistance.²

It is important to recognize that only the lowest points on the access curve can be reached from the film boiling side, and only the highest can be reached from the nucleate boiling side. When the curve is triple-valued along the access line, the middle points cannot be reached. Thus *much of the transition zone was simply inaccessible to Berenson, and he had no legitimate way of*

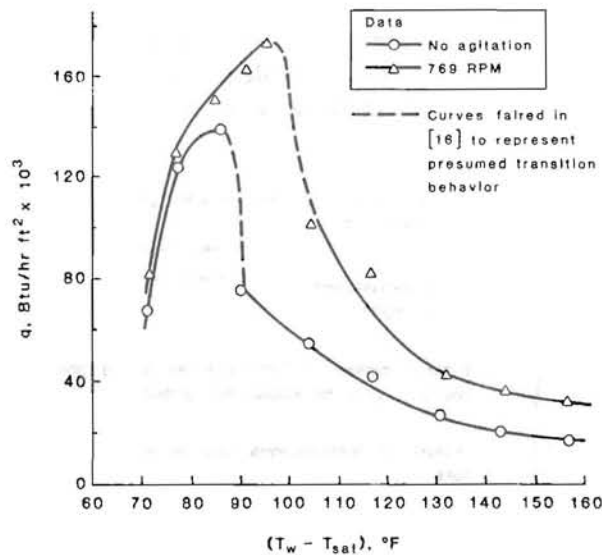


Fig. 6 Two of Pramuk and Westwater's boiling curves for saturated methanol on steam-heated horizontal copper tubes (one for still, and one for agitated, fluid) showing true transition boiling data. (We believe that the dashed portions of the curves are only speculative.)

² The neglect of the condensing resistance is conservative. It would actually make the access line less steep and more of the curve inaccessible.

inferring that a continuous path really existed. So it is clear that Kuhn's principle was at play in these early studies of transition boiling. These studies were done by experimentalists of unquestioned ability and integrity in the best-equipped laboratories of the day. Yet they (and we ourselves) all saw the transition boiling behavior that Nukiyama had first said they should see. Even to this day, many boiling specialists would accept either the notion that the transition boiling regime is a single continuous process, or that it is made up of a coexisting mixture of film and nucleate boiling.

The issue that lies within the question as to whether or not the curve is continuous is the question as to whether or not the transition boiling process itself is continuous. This question is at the root of the formulation of the Zuber-Tribus theory.

2.4. Precursors to the Zuber-Tribus Theory

In the late 1930's Bonilla, Drew, and Cichelli /19,20/ made a series of measurements of q in nucleate boiling up to q_{\max} , with q as the independent variable. These experiments were done in water and various organic liquids on a large horizontal flat plate under well-controlled conditions. Although the role of geometry in the problem was not diagnosed until many years later, these formed the first large data set that was free from geometrical effects or other serious systemic complications.

Bonilla and Perry /19/ include one modest observation in their paper

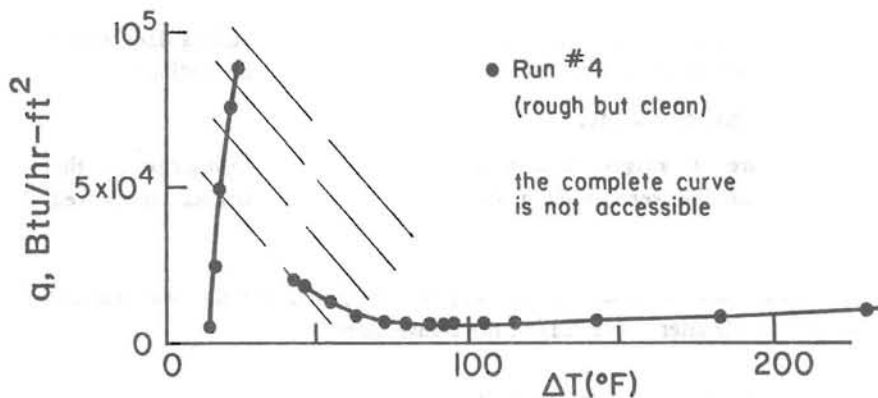


Fig. 7 Berenson's boiling run #4 for n-pentane on copper. Solid lines are our faired curves. Dashed lines represent accessibility curves in accordance with equation (2).

which we believe should be taken as the starting point for the hydrodynamic theory of boiling. They say:

“As film boiling is similar in effect to column flooding, a similar type of correlation may hold. In Figure 20 our maximum boiling rates are plotted on a column flooding correlation.”

Their “Figure 20” shows burnout data correlating within a factor of two on the following coordinates:

$$\frac{v_g^2 \rho_g}{2g\rho_f L} = f(\rho_f/\rho_g) \quad (3)$$

where³ v_g is the rate of vapor outflow and liquid inflow (at the peak heat flux) averaged over the heater area, and L is a characteristic dimension which they related to a Jakob prediction of the escaping bubble diameter.

There is much to criticize today (on the basis of a much better understanding of the vapor dynamics during boiling) about the way in which Bonilla and Perry drew the analogy between the peak, or “burnout” heat flux and the flooding of a distillation column. Nevertheless, *their perception that the escape of vapor from a heater during boiling will strangle the inflow of liquid in the same way that it will in a distillation column, is at the heart of the hydrodynamic theory of burnout.*

Yet this observation was not just ignored. It was actively opposed by two of the greatest chemical engineers of that day /21/. A.P. Colburn wrote to him:

“A correlation [of the flooding velocity plots with] boiling data would not serve any great purpose and would perhaps be very misleading.”

and T.H. Chilton also wrote:

“I venture to suggest that you delete from the manuscript ... the relationship between boiling rates and loading velocities in packed towers.”

Although the correlation did appear in print, Bonilla was clearly discouraged. He later wrote /21/ of the transaction:

“... I dropped further effort in finding a model ... that would be more ‘scientific’. ... It seems to me that a substantial number of professors, etc.

³ Symbols not defined in context are conventional ones. They are defined in the **Nomenclature**.

saw my 'burnout' correlation, but just weren't convinced enough to use it."

In the late 1940's, Kutateladze (see, e.g. /22/) began studying boiling burnout (which he calls the "first boiling crisis") from the viewpoint that it must be similar to the "flooding" that occurs when a gas is forced up through a liquid. The 1952 revision of Kutateladze's 1949 book on two-phase heat transfer /6/ included three chapters on which Borishansky had collaborated. One of these, Chapter 10, reflects Borishansky's Candidate dissertation work on the dimensional analysis of the equations that would describe such flooding.

Kutateladze and Borishansky developed a large number of dimensionless groups. One was a dimensionless peak heat flux which was later named the Kutateladze Number, Ku . A comparison of Ku with the limited existing data revealed that it did not depend strongly on the other groups. Thus

$$Ku \equiv \frac{q_{\max}}{h_{fg} \rho_g^{1/2} [\sigma_g (\rho_f - \rho_g)]^{1/4}} \approx \text{constant} \quad (4)$$

If we recognize that v_g is equal to $q_{\max} / \rho_g h_{fg}$ and that $[\sigma/g(\rho_f - \rho_g)]^{1/2}$ is a characteristic dimension associated with capillary wave action in a liquid-vapor interface, then it is clear that Bonilla's dimensionless burnout heat flux (in equation (2)) is exactly Ku . Kutateladze, while he was aware of Bonilla's work, can probably not be blamed for missing this point which had, after all, been advanced almost as an afterthought in /19/.

While Kutateladze's correlation was recognized in Russia, it does not appear to have caught Western attention until the late 1950's when Zuber and Tribus recognized its significance. But two more bricks were to be put into place before they did so. One was the postwar work on interfacial instability, and the other was Chang's insight into its role in the boiling problem.

In 1957, Yan-po Chang /23/ advanced a radical analysis of natural convection from an infinite horizontal flat plate. He observed that boundary layer convection is driven by the thermo-convective instability above it. He then attempted to couple the potential flow above to the boundary layer flow below to complete the description of the flow.

While his use of thermo-convective instability theory did not convince students of natural convection, Chang concluded his paper by drawing attention to the shape of the liquid-vapor interface in film boiling (see Fig. 3). The interface, he notes, has to be the result of a thermo-convective

instability. He verified this by showing that the thermo-hydraulic wavelengths compare favorably with those observed in film boiling.

Chang was invited to a stay at UCLA just after he produced this paper. There he discussed his ideas with Myron Tribus and his student, Novak Zuber, who was developing his dissertation on the hydrodynamic processes in boiling. Zuber, an extremely bright Yugoslav emigrant – fluent in Russian – was exploring the recent Russian literature with more care than anyone in the United States had previously given it.

2.5. Interfacial Stability Theory Before WW-II.

Zuber and Tribus were well-connected in three new areas of information that put them in a strong position: Kutateladze's work, Chang's work, and the post-war advances in interfacial stability theory. These latter advances were founded on extremely strong work that dated from the 1870's.

They identified three unstable liquid-vapor interfacial instabilities: The instability of a cylindrical interface; the instability of a liquid-over-vapor interface; and the instability of a liquid and vapor moving in opposite directions parallel with their interface. Let us look at the development of the analysis of these instabilities.

Lord Rayleigh set the foundation for studying the instability of jets with his consideration of several configurations of capillary waves on jets. He first analyzed the problem in 1878 in the Proceedings of the London Mathematical Society /24/; however most of us read the considerably expanded version first published in the second edition of his Theory of Sound in 1896 /25/.

Figure 8 shows how axisymmetric waves lie on a jet. We decompose any surface disturbance into axial cosinusoidal waves of length, λ , with amplitude, α . The local deflection of the surface, r , then varies thus with the axial position, x :

$$r = R + \alpha \cos kx \quad (5)$$

where k is the wave number, $2\pi/\lambda$.

Rayleigh used the principle that the capillary energy of a system must be a minimum with respect to disturbances. He calculated the minimum wavelength for which an increase in amplitude would cause the surface energy to decrease. When this happens, the wave must continue growing until a droplet is nipped off. Another way of looking at the instability is to note that the tendency for circumferential surface tension to clamp down in the valleys and

release the peaks can no longer be compensated by the straightening effect of axial tension. The minimum wavelength at which this occurs was

$$\lambda_{R,c} = 2\pi R = \text{jet circumference} \quad (6)$$

where $\lambda_{R,c}$ denotes the *critical* Rayleigh unstable wavelength.

If there is a spectrum of disturbances in the jet surface, then a somewhat longer wave — the one that grows most rapidly — will actually emerge from the spectrum. We defer discussion of the details, and simply note that this wave corresponds with the value of kR that maximizes the function $kR[1 - (kR)^2]I_1(kR)/I_0(kR)$, where I_1 and I_0 are the zero and first order modified Bessel functions of the first kind. This yields

$$\lambda_{R,d} = 4.51(2R) \quad (7)$$

where the subscript “d” denotes the most rapidly growing, or most susceptible, or “most dangerous” wavelength. (Rayleigh also showed that $\lambda_{R,d}$ for a gas jet in a liquid is $6.48(2R)$.)

Figure 9 shows a typical example of Rayleigh breakup of a jet. The actual wavelength is on the order of $4.51(2R)$, but somewhat longer, since the actual wavelength that grows is never precisely $\lambda_{R,d}$ but some value near it.

Niels Bohr [26] also looked at the jet breakup problem in 1909 in a remarkably comprehensive experimental/analytical study. He included the influence of viscosity in the analysis, and showed that its influence was slight. The study was actually aimed, not at learning about jet behavior, but at using jet dynamics to measure the surface tension of water in a freshly created liquid interface. His value of σ was 73.23 dyne/cm at 12°C which is about one percent below today’s accepted range.

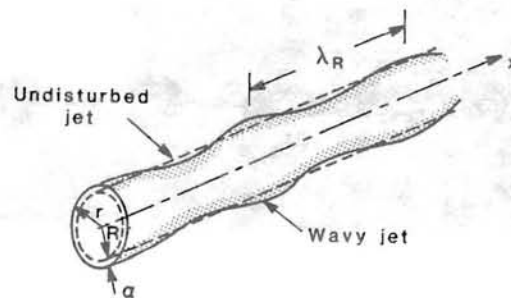


Fig. 8 Axisymmetric capillary waves in the surface of a jet.

Lamb /27/ expanded Rayleigh's analysis to treat circumferential waves as well as axisymmetric ones, in 1932. Rayleigh had acknowledged the possibility of such waves, but neglected them in his solution. Lamb analyzed them but showed them to be stable.

Harrison /28/ studied the motion of a plane interface between a heavy fluid beneath, and a lighter one above, in 1908. However, both Lamb and Harrison were concerned with formulating correct equations for the interfacial motion rather than with the waves, once they were formed. Harrison included influences of viscosity and surface tension and showed that for a system such as air over water, the influence of surface tension dominates over that of viscosity – particularly at shorter wavelengths. But his handling of viscosity was admittedly inaccurate for shorter waves.

2.6. Early Post-War Formulations

In 1950 Taylor published his famous paper /29/ on the *instability* of liquid interfaces between two superposed fluids of differing densities, with a body force acting normal to them. He included neither viscosity nor surface tension in his analysis. What he did was really quite simple and it drew upon the work of Lamb and Harrison.

A Formulation of the Interfacial Stability Relations Applicable to the Present Review. We shall briefly develop the basis for Taylor's instability analysis, greatly expanding his model to include surface tension, flow parallel to the fluid-fluid interface, and some limited three-dimensionality. This way we shall

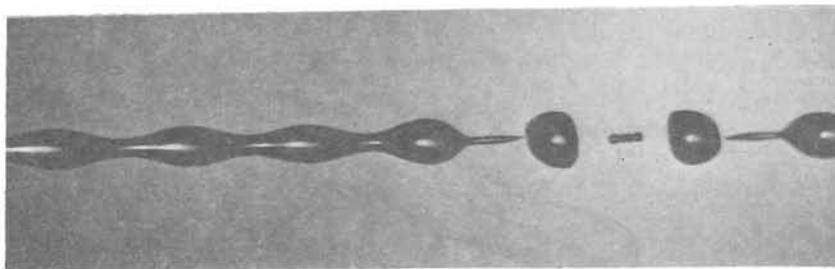


Fig. 9 A typical example of Rayleigh breakup in a 1.3 mm diam. water jet moving from left to right in air. $\lambda_{\text{H}}/2R = 4.7$.

have the apparatus that is needed to discuss other interfacial stability cases we must deal with subsequently. We shall then return to the thread of our historical account.

A traveling wave in the interface between one fluid (whose properties are identified with a prime) on top, and a second fluid (whose properties are not primed) on the bottom, is shown in Fig. 10. The upper and lower layers of fluid are taken to have depths of h' and h , respectively. We consider disturbances of the following form in the interface:

$$\eta = \alpha \exp [i(\omega t - kx)] \tag{8}$$

where ω is the frequency of the disturbance, and a is its amplitude. For real ω , the real part of this is the conventional traveling wave

$$\eta = \alpha \sin(kx - \omega t) \tag{9}$$

The complex potentials for this flow are well-known (see e.g. /30/). At the interface they yield the following potential and stream functions:

$$\phi = \alpha c \cos(kx - \omega t) \cosh ky \tag{10}$$

and

$$\psi = -\alpha c \sin(kx - \omega t) \sinh ky$$

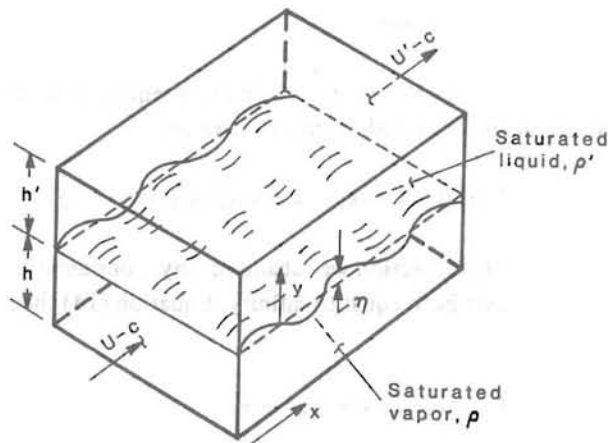


Fig. 10 A sinusoidal disturbance in the interface between two fluids. (The fact that the fluids are represented as saturated liquid above saturated vapor, in the picture, does not restrict analyses to this configuration.)

where c is the phase speed, ω/k .

We next set the interface at rest in Fig. 10, by subtracting the phase speed from each flow. The complex potential for the upper and lower flows in this configuration are /30/:

$$\begin{aligned} W' &= -(U' - c)z - \frac{\alpha(U' - c)}{\sinh(kh')} \cosh(z - ih') \\ \text{and} \\ W &= -(U - c)z - \frac{\alpha(U - c)}{\sinh(kh)} \cosh(z + ih) \end{aligned} \quad (11)$$

Equation (9) reduces to $\eta = \alpha \sin(kx)$ in this shifted coordinate frame, and the velocities of the upper and lower fluids at the interface can be expressed by:

$$\begin{aligned} u'^2 &= (U' - c)^2 [(1 + 2k\eta)\coth(kh')] \\ \text{and} \\ u^2 &= (U - c)^2 [(1 - 2k\eta)\coth(kh)] \end{aligned} \quad (12)$$

where terms on the order of α^2 or higher have been neglected.

Substituting equations (12) in the Bernoulli equations,

$$\begin{aligned} p' + \rho' u'^2/2 + \rho' g\eta &= \text{constant} \\ \text{and} \\ p + \rho u^2/2 + \rho g\eta &= \text{constant} \end{aligned} \quad (13)$$

and subtracting one from the other we obtain an equation in η . Requiring terms of first degree in η to vanish identically, we get

$$\rho' k(U' - c)^2 \coth(kh') + \rho k(U - c)^2 \coth(kh) = g(\rho - \rho') \quad (14)$$

In the remainder of this section we abandon any consideration of finite depths, h and h' , and set both equal to infinity. Equation (14) then yields

$$\rho' k(U' - c)^2 + \rho k(U - c)^2 = g(\rho' - \rho) \quad (15)$$

We include the influence of surface tension with the help of the so-called pressure conditions at the interface, which are obtained from the Euler equation of motion (see e.g. /30/)

$$\begin{aligned}
 p' &= \rho'(-g\eta + \phi_t' + \phi_x' U') \\
 \text{and} \\
 p &= \rho(-g\eta + \phi_t + \phi_x U)
 \end{aligned}
 \tag{16}$$

where the subscripts t and x denote partial differentiation. The pressure difference, $p - p'$ is given by the Laplace relation,

$$p - p' = -[\sigma/R_{xy} + \sigma/R_{tr}] \tag{17}$$

The curvature R_{xy} in the x-y plane is given by $R_{xy} \simeq \partial^2 \eta / \partial x^2$ so long as we deal in small disturbances. R_{tr} is the transverse curvature normal to the x-y plane.

We can write the complex potentials at the interface — analogous to equation (10) — in the shifted coordinates and for infinite depths, as

$$\begin{aligned}
 \phi' &= -i(U' - c) \alpha \exp[-ky + i(\omega t - kx)] \\
 \text{and} \\
 \phi &= i(U - c) \alpha \exp[ky + i(\omega t - kx)]
 \end{aligned}
 \tag{18}$$

Substituting equations (17) and (18) in the pressure condition, equation (16), we obtain (after rearranging the result and substituting $c = \omega/k$)

$$\begin{aligned}
 c &= \underbrace{\frac{\rho U + \rho' U'}{\rho + \rho'}}_i \\
 &\pm \sqrt{\underbrace{\frac{g(\rho - \rho')}{k(\rho + \rho')}}_{ii} + \underbrace{\frac{k\sigma}{\rho + \rho'}}_{iii} - \underbrace{\frac{\sigma}{k(\rho + \rho')R_{tr}\eta}}_{iv} - \underbrace{\frac{\rho\rho'(U - U')^2}{(\rho + \rho')^2}}_v}
 \end{aligned}
 \tag{19}$$

The physical significance of the five terms on the right-hand side of equation (19) is as follows:

- (i) is the mass mean velocity of the two flows.
- (ii) is the gravity term. If the heavy flow is below the lighter one, it tends to smooth out disturbances, and vice versa.
- (iii) is the axial curvature term. It acts to smooth out disturbances in either case.
- (iv) is the transverse curvature term. It can either oppose or augment the disturbances depending on whether or not it is in phase with the axial

curvature. The negative sign shown is for a disturbance that destabilizes the interface when η is negative.

(v) is the inertia term. It is the only term that Taylor considered and it augments the disturbances. (Taylor did not produce equation (19), and it includes terms that he did not include in his analysis.)

We are now primarily interested in the stability of waves and that stability turns on whether or not disturbances grow without bound. A wave of the type

$$\eta = \alpha \exp(-ikx + \omega t) = a \exp(-ikx + kct) \quad (20)$$

will grow without bound when c , as given by equation (19), has a negative imaginary component. This will occur when the argument of the negative radical is itself negative.

The value of wave number, k , (or wavelength, λ) for which the quantity under the radical turns from positive to negative is the "critical" value, k_c or λ_c — the shortest disturbance that can be unstable. The wavelength for which $\omega = kc$ has its maximum negative imaginary component is the "most susceptible" or "most dangerous" wavelength, $\lambda_d = 2\pi/k_d$. The wavelength that we normally expect to see grow in a real interface is λ_d , since it is the one that will most rapidly emerge from a Fourier spectrum of sinusoidal waves that make up any real disturbance in an interface.

Taylor, Rayleigh and Helmholtz Instabilities. Let us look at Taylor's prediction in which U and U' were zero; there was no transverse curvature, R_{tr} ; and no surface tension. In this situation, only term (ii) survives in equation (19) and it will be negative for all positive values of λ or k when $(\rho - \rho')$ is negative — when the heavier fluid is on top. Thus k_c is zero.

To obtain k_d we maximize ω by multiplying the radical by k , and equating the derivative of the result with respect to k to zero. The derivative is unfortunately $\frac{1}{2}[g(\rho - \rho')/k(\rho + \rho')]^{1/2}$, in this case, so it has no maximum. The longer the wavelength is, the more rapidly it grows.

Lewis /31/ conducted companion experiments for Taylor's paper in which he used an air drive to create downward accelerations, g_1 , of up to 50 times earth normal gravity in tanks of water and air, water and benzene, water and CCl_4 , and air and glycerin. His observation of the resulting wave growth

showed that Taylor's linearized exponential growth model was only valid as long as

$$\eta_{\max} \text{ or } \alpha < 0.4\lambda \quad (21)$$

Beyond an amplitude of 0.4λ , growth must be described by a non-linear analysis which becomes prohibitively complicated.

Lewis also observed that the instability of air-glycerine surfaces developed slightly faster than predicted by the linearized theory, although the growth of the waves followed the linear theory further than the less viscous fluids. This meant that high viscosity might play a role in the process.

Just a few years later, Bellman and Pennington [32] extended the analysis to include viscosity and surface tension. They found that viscosity opposes the tendency for disturbances to grow without bound — particularly those with shorter wavelengths, but that it does not remove instability for any wavelength.

On the other hand, Bellman and Pennington

“...expected that ... surface tension will remove the instability for sufficiently small wavelengths.”

And they showed that this was indeed the case. The inclusion of surface tension had the effect of retaining terms (ii) and (iii) in equation (19). Thus

$$c = \sqrt{\frac{g(\rho - \rho')}{k(\rho + \rho')} + \frac{\sigma k}{\rho + \rho'}} \quad (22)$$

Setting $ck = 0$, we obtain

$$\lambda_c = \frac{2\pi}{\sqrt{\frac{g(\rho - \rho')}{\sigma}}} \quad (23)$$

and setting the derivative of ck with respect to k equal to zero, we find

$$\lambda_d = \sqrt{3} \lambda_c \quad (24)$$

We include, in Fig. 11, Bellman and Pennington's frequency-wave-number relationship — called a “dispersion relation” — for an air-glycerin system with

$(g_1 - g) = 200 \text{ m/s}^2$, illustrating the influences of viscosity and surface tension.

One may also obtain Rayleigh instabilities from equation (19). Using the fact that in this configuration (Fig. 8), $R_{\tau, \eta} = R^2$, the transverse curvature destabilizes the interface when η is negative and $(U' - U)$ and gravity are negligible, we immediately obtain equation (6) from terms (iii) and (iv) by setting $ck = 0$. However, when we differentiate ck and set the result equal to zero, terms (iii) and (iv) yield $\lambda_{H,d} = \sqrt{12}\pi R = 10.88R$ which exceeds the accurate value given by equation (7) by 21 percent.

Thus we note that equation (19) – for all its simplicity – is inaccurate when the depth of a fluid (with substantial inertia) is finite, as it is inside a liquid jet. This limitation will not trouble us in the cases we look at subsequently.

Kelvin and Helmholtz were the first to examine the instabilities that result when $(U' - U)$ is not zero. Lord Rayleigh observed in his 1878 paper [24/ that

“...Helmholtz remarks upon the instability of surfaces separating portions of fluid which move discontinuously, and Sir W. Thompson [Lord

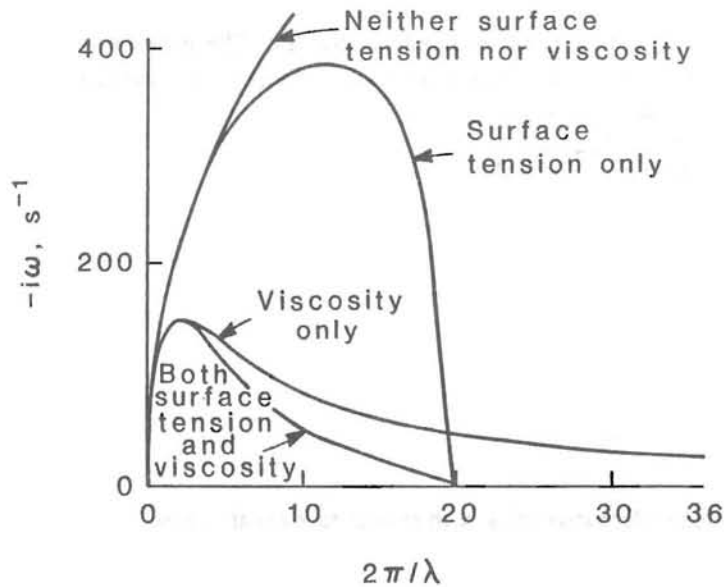


Fig. 11 Bellman and Pennington's dispersion relations for an air-glycerin system accelerated at 200 m/s^2 , illustrating the relative roles of surface tension and viscosity.

Kelvin], in treating of the influence of wind on waves in water, supposed frictionless, has shewn under what conditions a level surface of water is rendered unstable.”

Rayleigh goes further to say that his analysis of jet instability draws basically upon the prior work of Lord Kelvin.

A typical example of Kelvin-Helmholtz instability can be obtained by ignoring gravity (term (ii)) and transverse curvature (term (iv)), and setting $(U - U') = U$. The results are:

$$\lambda_{H,c} = \frac{2\pi(\rho + \rho')\sigma}{\rho\rho'U^2} \quad (24)$$

and

$$\lambda_{H,d} = \frac{3}{2} \lambda_{H,c} \quad (25)$$

We shall subsequently be interested in the minimum velocity needed to render a disturbance of known wavelength unstable when a low density vapor (ρ') passes a near stationary liquid of relatively high density (ρ). This would be the critical Helmholtz velocity based on the critical Helmholtz wavelength,

$$U = \sqrt{\frac{2\pi\sigma}{\rho\lambda_{H,c}}} \quad (26)$$

One can readily calculate other instabilities with the help of equation (19) – the combined influence of parallel flow and gravity, with or without surface tension, for example. Thus, once Taylor had set the strategy for analyzing instabilities, a variety of additional instability calculations followed rapidly. The fairly comprehensive collection of Helmholtz instability solutions given us by Haggerty and Shea /33/ as early as 1955 illustrates how rapidly this new means of analysis was being embraced.

3. The Zuber-Tribus Model

3.1. Zuber's Set of Hydrodynamic Transitions

Zuber's dissertation is ^{an} ambitious document dealing with the entire problem of pool boiling. Its first two chapters dealt with nucleate boiling and bubble growth, and the last four virtually set the agenda for this review:

3. "Hydrodynamic Aspects of Nucleate Boiling"
4. "Hydrodynamic Aspects of Transition Boiling"
5. "The Minimum Heat Flux Density in Transitional Boiling from a Horizontal Surface"
6. "The Critical Heat Flux in Boiling From a Horizontal Surface"

Zuber argued convincingly in his third chapter that a significant hydrodynamic transition occurs in the nucleate boiling regime — a transition in which bubbles rising from a heater surface coalesce into vapor jets and columns. Boiling on either side of this transition is shown in photographs 4a and 4b in Fig. 4. The conduits of vapor outflow formed by the jets eventually become unstable and collapse causing burnout. This, in fact, is the basis of the flooding process suggested by Bonilla and articulated more precisely by Kutataladze.

But Zuber was not content just to *correlate* burnout data; he wanted to *predict* it as well. To do that he had to predict the size and spacing of the jets. The key to doing this, he recognized, lay in understanding the dynamics of vapor movement in the transition region, and this was the subject of his fourth chapter. The q_{max} and q_{min} predictions for which the dissertation is best known were then the subject of the last two chapters.

We defer consideration of the transition from the region of nucleate boiling to the region of jets (or slugs) and columns since, while Zuber had identified this transition, he did not try to predict it until later. We focus here on the peak and minimum transitions which Zuber approached through transition boiling.

3.2. Zuber's Diagnosis of Transition Boiling

Zuber studied Westwater's and Santangelo's /34/ photographs and descriptions of transition boiling. From them he formulated a model of transition boiling to serve the whole regime. His sketches for this model, reproduced in Fig. 12, show how he envisioned a liquid-vapor interface caving-in in a jet-like spike that explosively boiled before it touched the surface. The vapor, thus formed, created a mushroom bubble.

Figure 4c indeed shows this sort of behavior just as Westwater and Santangelo's photos did. However there were two misapprehensions involved in Zuber's description:

- The first was that he adopted Westwater and Santangelo's suggestion that there was no contact between liquid and solid during transition boiling.

Solid evidence to the contrary was not forthcoming until several years later.

- The second misapprehension was that a single mechanism characterized transition boiling. In fact, the photographs in /34/ include a picture of transition boiling somewhat above q_{\min} that perfectly resembles the film boiling we see in Figs. 4d and 12d and e; but it also includes a shot of the violent transition boiling of the kind shown in Figs. 4c and 12f.

These points, however, did not undercut Zuber's primary argument which was that the Taylor instability process set the basic behavior throughout the region. Since throughout this region the liquid above collapses into the vapor below, he proposed that the transition collapse mechanism had to be spaced on the Taylor wavelength — either λ_d or λ_c , he was not sure which. It followed that, as ΔT was increased and film boiling was established, this wavelength would have to mark the collapse of waves and the spacing of escaping bubbles in that region as well.

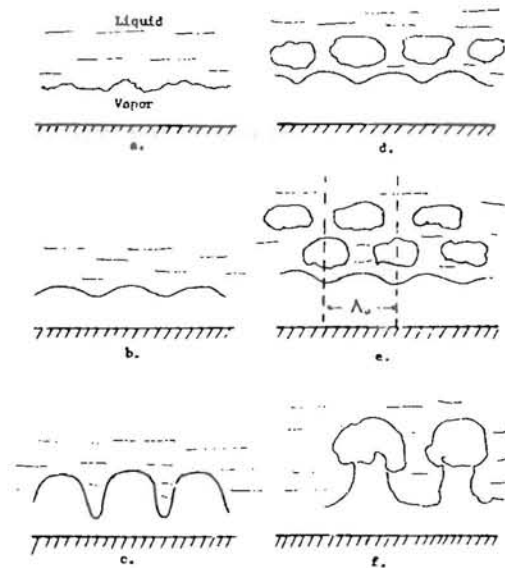


Fig. 12 Zuber's representation of transition boiling (from /2/). a., b., and c. show the evolution of the collapse of an interface from an initially disordered state; d. and e. show cyclic Taylor collapse near q_{\min} ; f. shows the violent boiling that follows condition c. at a much higher heat flux.

By the same token, he argued, as ΔT was reduced back over the peak heat flux and into the region of slugs and columns, the same λ_d would have to set the spacing of the escaping vapor jets.

3.3. Formulation of the q_{\max} Prediction

Figure 13 shows the idealized liquid-vapor interface, and it points out some difficulties that did not come to light for another 14 years. Zuber postulated that a two-dimensional array of waves collapsed cyclically in place. Thus the waves oscillated without traveling. Zuber correctly noted that the waves must form a square array (a hexagonal array of jets could not oscillate) and he made a marvelous pair of compensating errors:

He used Taylor's 1-dimensional wave formulations for both λ_d and λ_c , and he neglected to include the center jet that had to occupy the center of the square array. Not until 1969 did Sernas /35/ show that the 2-dimensional wavelength, $\lambda_{d,2}$, is larger than λ_d by a factor of $\sqrt{2}$ as shown in Fig. 13. The remarkable thing about this factor is that it made Zuber's presumed geometry take the form of the cross-hatched area in the figure; and this is a completely legitimate subset of the correct geometry.

Zuber also assumed — seemingly without sufficient cause — that the radii of the escaping liquid jets during nucleate boiling, and of the escaping bubbles during film boiling, were both equal to $\lambda_d/4$. It immediately follows that, for the geometry in Fig. 13, the ratio of jet area, A_j , to heater area, A_h , is

$$\frac{A_j}{A_h} = \frac{\pi}{16} \quad (27)$$

Burnout now occurs when the jets, as shown in Fig. 14, become Helmholtz unstable. To predict q_{\max} we begin by making an elementary energy balance that involves A_j/A_h . Equating the heat flux at burnout to the latent heat that escapes, yields

$$q_{\max} = \rho_g h_{fg} u_g \frac{A_j}{A_h} \quad (28)$$

where u_g is the limiting vapor velocity that causes the escaping jets to become Helmholtz unstable. Zuber took this to be the critical — not the most dangerous — Helmholtz wave, since the first wave that can collapse will do so.

Insofar as it is legitimate to neglect curvature in the jet wall and to assume that $\rho_f \gg \rho_g$, we can then use equation (26) for u_g .

The next serious problem that Zuber faced was that of specifying the unknown Helmholtz wavelength to use in equation (26). His choice was the critical Rayleigh wavelength, $\lambda_{R,c}$, which is given by equation (6) as $2\pi R$, where R is assumed to be $\lambda_d/4$ and λ_d is in turn given by equations (23) and (24). Using this result and equation (27) in equation (28), we obtain

$$q_{\max} = C \frac{\pi}{24} \rho_g h_{fg} [\sigma_g (\rho_f - \rho_g)]^{1/4} \tag{29}$$

where the constant, C , would be $3/\sqrt{2\pi} = 1.197$ if the critical wavelength were used and $3^{3/4}/\sqrt{2\pi} = 0.9094$ when the most dangerous wavelength is used. Since these numbers bracket unity, Zuber recommended using $C = 1$. This gave

$$Ku = \frac{\pi}{24} = 0.131 \tag{30}$$

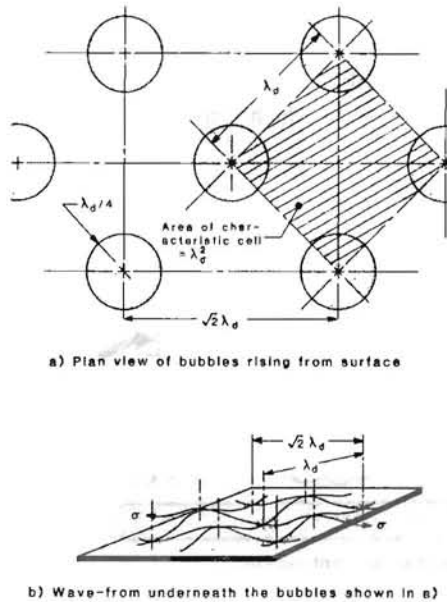


Fig. 13 The array of vapor jets as they are placed on an infinite horizontal surface.

Zuber thus flew in the face of convention when he argued that the lowest film boiling heat flux occurred when vapor was not produced rapidly enough to lift the liquid-vapor interface as rapidly as it would normally collapse. To predict q_{\min} he said, one had to predict the natural rate of collapse. His prediction then took the form:

$$q_{\min} = \left[\begin{array}{l} \text{latent heat} \\ \text{transport} \\ \text{per bubble} \end{array} \right] \left[\begin{array}{l} \text{bubbles} \\ \text{per wave} \\ \text{oscillation} \end{array} \right] \left[\begin{array}{l} \text{minimum number} \\ \text{of oscillations} \\ \text{per unit time} \end{array} \right] \left[\begin{array}{l} \text{waves per} \\ \text{unit area} \\ \text{of heater} \end{array} \right] \quad (31)$$

where the latent heat transfer per bubble is $\rho_g h_{fg} (2\pi/3) (\lambda_d/4)^3$ based on a bubble diameter equal to $\lambda_d/2$. There are clearly 2 bubbles per wave oscillation – one per half-cycle. And, of course, the number of waves per unit heater area is $1/\lambda_d^2$.

Determining the minimum number of oscillations per unit time is the difficult part of the calculation. Unfortunately, the rate of collapse grows as the wave grows, until a bubble breaks away and the cycle repeats. Since the interfacial stability theory described in Sections 2.5 and 2.6 is linear, the growth rate based upon it is only valid in the linear growth region. Zuber averaged the growth over the wave amplitude in the linear regime and attempted to extrapolate the result into the nonlinear range. The attempt was incorrect in both the averaging and the extrapolation. However, his result had the correct functional dependence upon the relevant variables.

$$\text{frequency} \sim [g(\rho_f - \rho_g)/\rho_f \lambda_d]^{1/2} \quad (32)$$

The resulting expression for q_{\min} was then

$$q_{\min} = C \rho_g h_{fg} [g(\rho_f - \rho_g)/(\rho_f + \rho_g)^2]^{1/4} \quad (33)$$

where Zuber computed C as $(\pi^2/60)(4/3)^{1/4}$. While Zuber had access to the data set upon which Kutateladze's empirical q_{\max} prediction was based, he had no such information for q_{\min} at his disposal. He compared equation (33) with an isolated data point from Westwater and Santangelo [34], with inconclusive success. However, the data point represented a horizontal cylinder and not a flat plate.

3.5 Early Reactions to the Hydrodynamic Theory

Some problems with the theory. New theories, if they have any substance, are seldom correct in all their details. Darwin's evolution trees had to be

emended, Planck incorrectly took the energies of photons to assume a range of values, and Einstein failed to account for the contributions of coupled vibrations to the specific heat of metals. We count eight basic problems with Zuber's formulation:

1. The transition region does not actually represent a single continuous phenomenon.
2. Liquid in fact contacts the solid in the transition region.
3. The correct Taylor wavelength above a flat plate must be specified by a 2-dimensional analysis instead of a 1-dimensional one.
4. He omitted the center jet that had to oscillate against the four corner jets.
5. He used an incorrect averaging-technique to establish the frequency of escaping bubbles during film boiling.
6. In several places he either did not know whether to use the most-dangerous, or the critical, wavelength; or he was unclear as to the reasons for choosing one or the other.
7. Zuber's use of the Rayleigh wavelength in the escaping jet is probably incorrect — at least in most cases.
8. He presumed that both the jets in nucleate boiling and the bubbles in film boiling had radii of $\lambda_d/4$, which seemed arbitrary.

Not all of these failings were evident at the time. In fact, many of them *could* not have been evident, since later experiments would be needed to show that they were failings. Consequently they were challenged piecemeal — often by people more interested in proving the theory incorrect than in plumbing its possibilities.

Some Initial Reactions to the Theory. The literature of the early 1960's makes it clear that the initial challenge to the Hydrodynamic Theory of Boiling revolved about its failure to make provisions for any influences of heater-surface characteristics.

Just one year after Zuber's thesis Bernath /36/ captured people's attention with a paper that provided a variety of q_{\max} measurements on heaters of different sizes, heating-element thicknesses, and surface conditions. The values, of course, exhibited wide variability. Zuber had really failed to drive home the point that his q_{\max} model was only applicable to infinite, horizontal, isothermal heaters; and Bernath failed to provide means for isolating the influence of surface condition from the other variables that he investigated.

Consequently, Bernath's thought-provoking results became a focus of the attention of many who distrusted Zuber's model. Chang himself was an early critic of Zuber's model: Though he had first pointed out the presence of Taylor waves in film boiling; and though he had advanced a discussion of the relation of the Taylor process to film boiling /37/ three months before Zuber's thesis was published; he nevertheless did not subsequently credit Zuber's stability arguments in relation to q_{\max} and q_{\min} .

In 1962, Chang /38/ advanced a set of hypotheses as to the cause of burnout, all of which involved the surface heavily in the process. Although he pointedly does not cite Zuber, the work is a clear challenge to the Hydrodynamic Theory. Even more pointed is Costello's published discussion which appears with the paper. Costello also avoids referencing Zuber, but he says:

"I would like to compliment Dr. Chang on a realistic approach to the problem of burnout and also on clearly stating factors which might give use [sic.] to nonhydrodynamic effects."

Charlie Costello was probably the most vigorous opponent of the theory. He was a boiling experimentalist who (we all learned in 1965) had been working under the early death sentence of terminal diabetes. His technical career was brief and intense. He was dedicated to his students, his research, and charitable works. He left us with a disturbing, and eventually useful, legacy of data and unanswered questions about burnout. And he plunged himself into the controversy with a fey kind of verve.

The title of his 1963 paper with Frea /39/, "A Salient Non-Hydrodynamic Effect on Pool Boiling Burnout of Small Semi-Cylindrical Heaters," very clearly trumpeted the general theme of his and Chang's challenge of the theory. It called into evidence several experiments showing surface effects on q_{\max} . His q_{\max} data for full and half cylinders of three sizes, in tap and distilled water, fresh and aged, with and without a wetting agent, showed wide variability. The problem of course, was that there, as in Bernath's earlier work, the various influences were not sorted out systematically.

Indeed, those of Costello's results that have subsequently been studied in the light of more complete statements of the hydrodynamic theory have been found consistent with it, as we see in Section 4.5. However, his criticisms, more than anyone else's, caused people (particularly in the Chemical Engineering heat transfer community) to turn away from the Zuber-Tribus formulation.

One of Costello's last works indicated that he was among the first to see

the reason — beyond surface influences — that many of the previous experiments gave such variable results. Titled “The Interrelation of Geometry, Orientation, and Acceleration in the Peak Heat Flux Problem,” the work /40/ hinted at what dimensional analysis would eventually make clear — that a proper scaling of q_{\max} would show that it depended on a parameter involving both size and gravity, for a given configuration.

4. Subsequent Articulations of the Zuber-Tribus Theory

4.1. Berenson’s Transition Boiling Study

While a fairly noisy argument raged over the hydrodynamic theory, certain formidable allies recognized that there must be something to this new set of ideas. At the 1961 International Heat Transfer Conference, Westwater joined with Zuber and Tribus in an extension of the work to include subcooled boiling /3/; and a year later Westwater and Breen /41/ used the Taylor wavelength as the scaling parameter for film boiling on small cylinders.

Berenson also worked quietly on the theory at MIT. His important doctoral dissertation /17/ was *critical* of the theory, but in the most positive sense of the word. It was the first study to systematically identify and resolve any of the problems we listed in Section 3.5. The dissertation involved an experimental-analytical study of transition boiling using the apparatus depicted in Fig. 15, which we discussed in Section 2.3 in our discussion of the accessibility of transition boiling points.

This experiment produced burnout data for CCl_4 and n-pentane on a flat plate between 3 and 4 times λ_d in diameter — large enough to admit legitimate comparison with an infinite plate theory. The data were only slightly higher than the theory predicted. The experiment also showed that great variations in surface finish influenced q_{\max} less than ± 10 percent *in a comparison in which other factors were held constant*. The critics at this point viewed even this small influence as incrimination, while supporters were quite willing to accept it as support.

Berenson showed that the influence of surface condition took two forms — an influence of roughness which was relatively minor beyond the nucleate boiling regime, and an influence of “surface chemistry” (by which we should probably understand “contact angle”) which was a very important factor in the transition boiling regime. A low contact angle signifies that the liquid can more easily “wet” the surface.

Figure 16 shows two typical Berenson boiling curves for one surface-liquid

combination, and one roughness. In one case the surface is clean and reasonably unwetted. In the other it is slightly oxidized with much better wetting characteristics. In hindsight we see that the transition boiling region was largely inaccessible on the very clean heater, except at very low heat fluxes; and entirely accessible – with far higher heat fluxes – when the surface was wetted.

But of particular importance was the fact that changing the chemical condition of the surface radically altered q_{\min} . Thus, Berenson argued, the Zuber q_{\min} prediction ought to be viewed as an *ultimate* minimum – one that can readily be exceeded by surface contacts when the liquid is allowed to wet the heater.

Berenson reconstructed Zuber's q_{\min} prediction, retaining all of its features except the prediction of the minimum bubble frequency. While Zuber had created an amplitude-average of the wave growth, Berenson

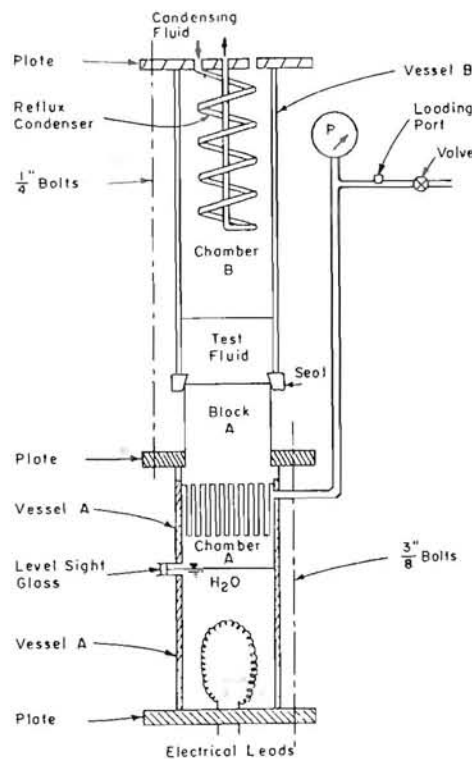


Fig. 15 Berenson's /17/ apparatus.

recognized that such an average could not correctly be made using a linearized, small-amplitude, theory. Zuber's η -average had to be replaced with a time-average. But to make a time average, one must not only know the course of the nonlinear portion of growth, he must also know the amplitude of the disturbance at $t = 0$. This meant that equation (33) was correct, but that neither Zuber nor anyone else could correctly establish the constant, C , from first principles.

Berenson compared equation (33) with two data points that seemed to represent true minima and concluded that C should be 0.09 — about half of Zuber's value of 0.177. This meant that someone else's experiment might later yield an even lower value and it sowed doubt about the issue of predicting q_{\min} .

4.2. The Zuber-Moissis-Berenson Transition

Only two years later Moissis and Berenson /42/ picked up on another hydrodynamic transition whose existence was originally suggested by Zuber.

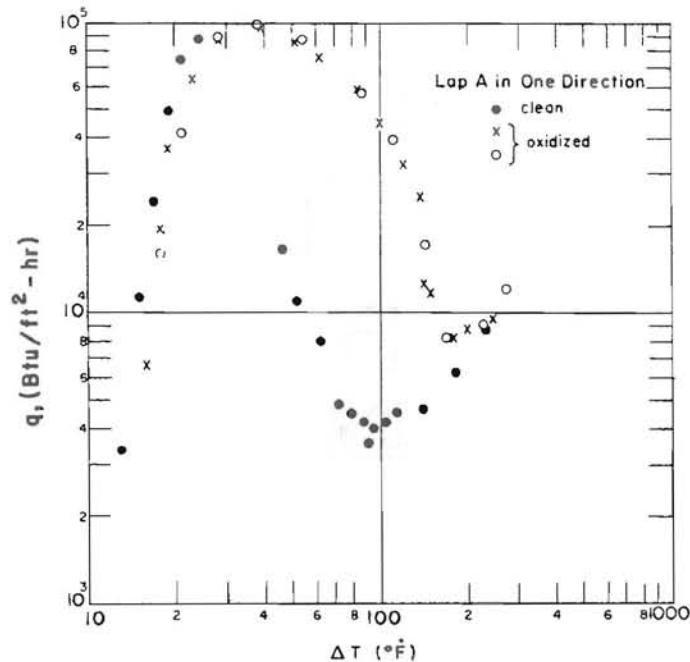


Fig. 16 Berenson's /17/ data for n-pentane boiling on a roughened copper surface — both clean and oxidized.

Zuber had noted in /2/ that there must be a transition from one nucleate boiling mechanism in which the bubbles are isolated from one another to another mechanism in which the bubbles merge to form jets and columns. a few years later he /43/ expanded this notion to predict the transition. We briefly summarize the Moissis-Berenson form of this prediction.

The assumed mechanism of the transition is simple: As the nucleate boiling heat flux is increased, isolated bubbles rise with increasing frequency from each active site. When they become close enough together to touch one another, a vapor jet must replace the series of bubbles. The point where this occurs depends on the departure diameter of the bubbles, and that in turn depends on the contact angle, β . Thus the transitional heat flux, q_{MB} , obtained in /42/ for a flat plate heater, was:

$$q_{MB} = 0.11 \rho_g h_{fg} [\sigma g / (\rho_f - \rho_g)]^{1/4} \beta^{1/2} \text{ (flat plate)} \quad (34)$$

Zuber's /43/ slightly simpler prediction of the transition did not involve the contact angle, but it approached equation (34) at low pressures. Instead of the lead factor $0.11\beta^{1/2}$, he got $1.53\pi/6$, which yielded a favorable comparison with the data of Gaertner and Westwater /44/. The two lead factors are equal when β is 53° , and it turns out that 53° would be a plausible value for the data in /44/.

Lienhard and Bhattacharya /45/ rederived equation (34) in 1972 for a horizontal cylindrical heater of radius, R , and got:

$$q_{MB} \cong 0.000333 \rho_g h_{fg} \sqrt[4]{\frac{\sigma^3}{g(\rho_f - \rho_g)}} \frac{\beta^{3/2}}{R} \text{ (cylinder)} \quad (35)$$

Both equations (34) and (35) were verified experimentally, but the transitions were blurred over modest ranges of q . Both depend on β , which is a nuisance variable in the problem, but the flat plate prediction suffers far less, since q is proportional to $\beta^{1/2}$ instead of $\beta^{3/2}$.

As an interesting sidelight, in 1983 Nishikawa et al. /46/ observed nucleate boiling on a horizontal plate tilted through angles, θ , as shown in Fig. 17. His results, also shown in Fig. 17, reveal a most startling fact: As the heat flux is raised to q_{MB} (based on a contact angle experimentally shown /47/ to have lain between $\beta = 35^\circ$ and 65°), the influence of orientation vanishes.

The implications of this are discussed in /47/, but the fact that a radical change in mechanism occurs at q_{MB} , is inescapable. An important corollary to this conclusion is that the myriad analyses of nucleate boiling based on

individual bubble action – long after Zuber’s original recognition of the transition – *cannot have any value* except at very low heat fluxes.

Equation (35) was developed as part of a study /45/ of the hydrodynamic transitions that occur, not in boiling, but in high current-density electrolysis. It was shown that, since there is no mechanism analogous to heat convection to enhance gas generation after the “slugs-and-columns” has been reached, the Zuber-Moissis-Berenson transition defines the maximum in this process. Figure 18 shows how the vapor flux, $v_g = q/\rho_g h_{fg}$, during boiling and the gas flux during electrolysis would compare. Photo insets show the electrolysis process near the limiting $v_{g,MB}$ and in the film region.

4.3. Film Boiling on a Horizontal Cylinder

Lienhard and Wong /48/ provided the first attempt to verify any element of the hydrodynamic theory by direct observation *in situ*, at about the same time that Moissis and Berenson were doing their work. Wong conducted a photographic study of film boiling near q_{min} on small horizontal cylindrical heaters of various sizes and measured the Taylor unstable wavelengths. The

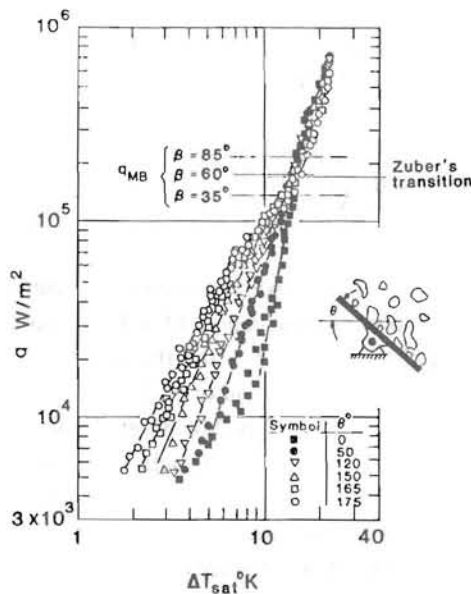


Fig. 17 The data of Nishikawa et al. /46/ and the predicted transition from isolated bubbles to slugs-and-columns.

Vapor or gas volume flux (or superficial velocity), v_g , $m^3/m^2 - s$

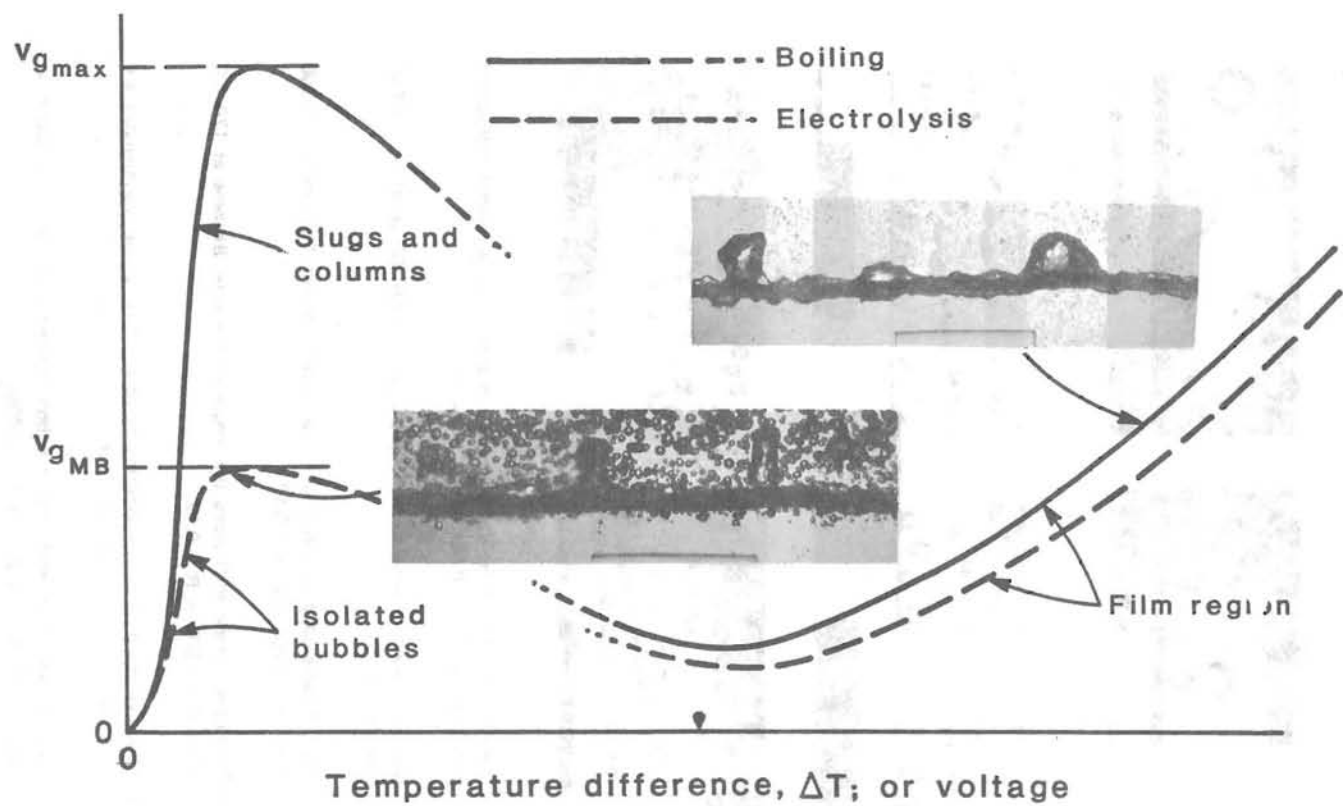
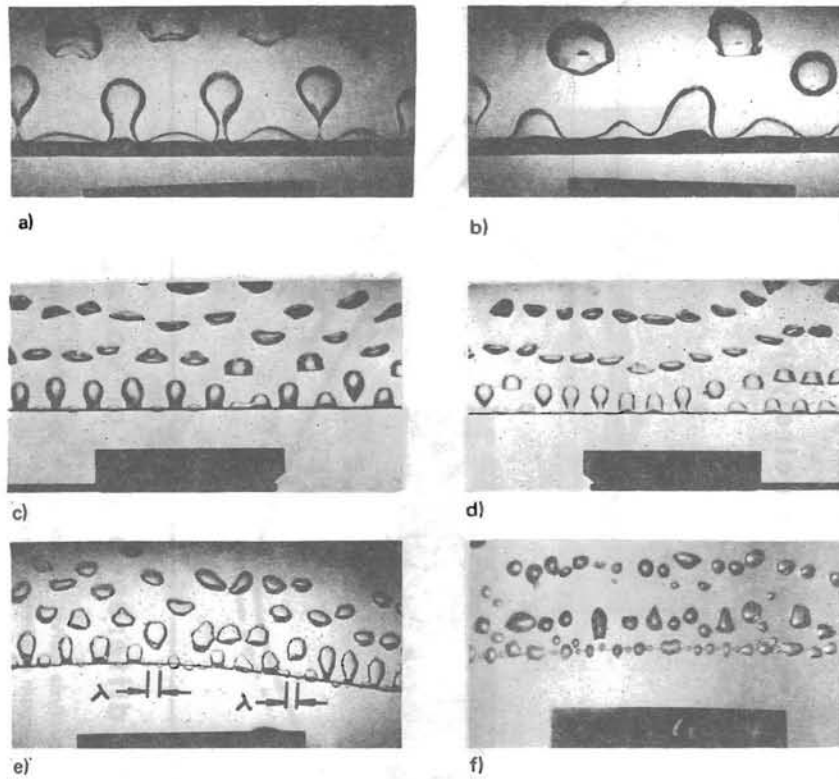


Fig. 18 Schematic boiling and electrolysis curves. Photo inserts show high-current electrolysis near the local maximum and in the film region.

J.H. Lienhard and L.C. Witte

Reviews in Chemical Engineering



- a) Clean bubble departure. Bubbles nearly in phase with each other. Isopropanol at $50,400 \text{ W/m}^2$, $R = 0.645 \text{ mm}$, $R' = 0.425$
- b) Typical imperfect wave pattern. Isopropanol at $50,400 \text{ W/m}^2$, $R = 0.645 \text{ mm}$, $R' = 0.425$.
- c) Clean bubble departure with one clear bubble merger. Benzene at $170,000 \text{ W/m}^2$, $R = 0.200 \text{ mm}$, $R' = 0.12$.
- d) Continuous phase shift along the length of the wire. Benzene at $170,000 \text{ W/m}^2$, $R = 0.200 \text{ m}$, $R' = 0.12$.
- e) Extensive merging of neighboring bubbles. Two actual wavelengths are identified. Isopropanol at $374,000 \text{ W/m}^2$, $R = 0.814 \text{ mm}$, $R' = 0.0535$.
- f) Wave behavior completely lost in bubble mergers at low R' . Isopropanol at 1.42 MW/m^2 , $R = 0.0127 \text{ mm}$, $R' = 0.0084$.

Fig. 19 Various bubble departure patterns from horizontal wires from /48/. Black marker is a 2.54 cm reference scale.

results showed that λ_d was a strong function of the heater diameter. Figure 19 shows a typical set of these photographic results.

The vapor film behavior in this case clearly has elements akin to both the Rayleigh instability of a jet and the Taylor instability of a heavy fluid above a lighter one. We accordingly go to equation (19) to identify the elements that Lienhard and Wong used to analyze this configuration. These are the Taylor gravity term, (ii), the Bellman-Pennington axial surface tension term, (iii), and the simplified Rayleigh transverse curvature term, (iv).

The trickiest part of this analysis was that of writing the transverse curvature term. The fact that the configuration is approximated as planar has subsequently been justified. It is also legitimate to use the deep-fluid approximation built into term (iv) since the fluid inertia lies almost entirely in the external liquid. Lienhard and Wong then took the transverse curvatures of the interface to have the form shown in Fig. 20, based upon photographs such as Fig. 19 and Fig. 4d.

The problem then reduces to identifying $1/\eta R_{tr}$ in term (iv). We note that the fluctuation of R_{tr}^{-1} has an amplitude that is only half the amplitude of η , and opposite to it in sign. Thus

$$(\eta R_{tr})^{-1} = \frac{1}{2\eta} \frac{\partial^2 \tilde{\eta}}{\partial x^2} = k^2/2R^2 \tag{36}$$

Equation (19) then gives the dispersion relation

$$\omega = \left[-kg \frac{\rho_f - \rho_g}{\rho_f + \rho_g} + \frac{\sigma k^3}{\rho_f + \rho_g} - \frac{\sigma k}{2(\rho_f + \rho_g)R^2} \right]^{1/2} \tag{37}$$

Setting ω equal to zero, we then get $\lambda_c = 2\pi/k_c$:

$$\lambda_c = \frac{2\pi}{\sqrt{\frac{g(\rho_f - \rho_g)}{\sigma} + \frac{1}{2R^2}}} \tag{38}$$

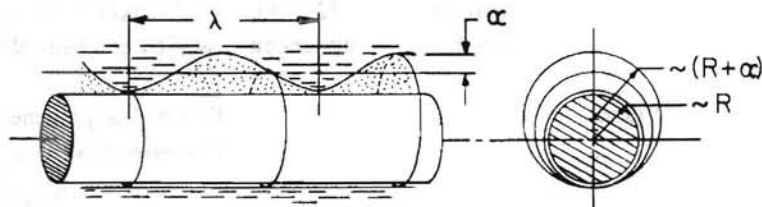


Fig. 20 The assumed geometry /48/ of film boiling on a horizontal cylindrical heater.

and setting the derivative of $\omega = 0$, we obtain

$$\lambda_d = \sqrt{3} \lambda_c \quad (39)$$

just as we did for the Bellman-Pennington stability problem.

These expressions were successfully compared with data in /48/. However, the comparison seemed to show that they slightly under-predicted the data. In 1969 Sun and Lienhard /49/ cast further light on this matter when they plotted dispersion relations, given by equation (37), for the system (see e.g. Fig. 21). In this case R , ω , and λ_d have been nondimensionalized in the form

$$R' \equiv \frac{R}{[\sigma/g(\rho_f - \rho_g)]^{1/2}} \quad (40)$$

$$\Omega \equiv i\omega[\sigma/g^3(\rho_f - \rho_g)]^{1/4} \quad (41)$$

and

$$\Lambda \equiv \frac{\lambda_d \text{ for a cylinder -- equation (38)}}{\lambda_d \text{ for a flat plate -- equations (23/39)}} \quad (42)$$

The group R' is an important one. It arises often in what follows. Sometimes called a Laplace number, it characterizes the relative importance of buoyant forces with respect to capillary forces. ($(R')^2$ is called a Bond number.) When R' (or more generally L' , where L is a general characteristic length) is on the order of 0.1 or less, we can expect capillary forces to control the bubble departure. This is what happens in Figs. 19-e. and 19-f. where R' is 0.0535 and 0.0084. At these low R' 's, the Taylor process deteriorates because bubbles merge before they can buoy away.

Figure 21 shows that there is typically a fairly broad band of wavelengths for which the frequency is within, say, 90 percent of its maximum value. Furthermore, this band is skewed toward values greater than λ_d . Figures 22-a and 22-b show the wavelength results from both /48/ and /49/ with the 90 percent wavelength band plotted in Fig. 22-b. Figure 22 makes it very clear that the observed scatter is very accurately encompassed by the band shown in Fig. 21, and that it is centered on equation (39).

Figure 22 (and equation (38)) also show that as $R \rightarrow \infty$, λ approaches the flat plate value, and for all practical purposes an R' greater than 2 or 3 is infinite. This does not mean that the vapor escape processes for q_{\max} and q_{\min} are to be taken as the same as on a flat plate. It only means that the transverse curvature (term (iv) in equation (19)) ceases to be influential.

4.4. Burnout on a Horizontal Cylinder

Dimensional Analysis and Corresponding States. Many investigators, however well convinced they might have been that the Taylor process applied in film boiling, found the Helmholtz collapse mechanism for burnout to be a far less digestible concept. Furthermore, throughout the 1960's very little was accomplished in the way of improving or expanding Zuber's q_{max} prediction. The chief way in which the idea *did* gain ground was through the increasing recognition that it was dimensionally sound.

If we note that equation (29) depends solely on the thermodynamic variables, σ , ρ_f , ρ_g , and h_{fg} , and the single system variable, g , then it is clear that it should be subject to Corresponding States correlation. Such correlations emerged simultaneously from Russia /50/ and the United States /51, 52/ in 1961. The formulation given in /51, 52/ used the Parachor, P , to eliminate surface tension, whence equations (4) and (29) for q_{max} , and equation (33) for q_{min} , all took the form:

$$q_{max}/\chi \text{ or } q_{min}/\chi = f(p_r) \tag{43}$$

where p_r is the reduced pressure, p/p_c , and

$$\chi \equiv p_c g^{1/4} \frac{P}{M} \frac{8Mp_c}{3RT_c} \tag{44}$$

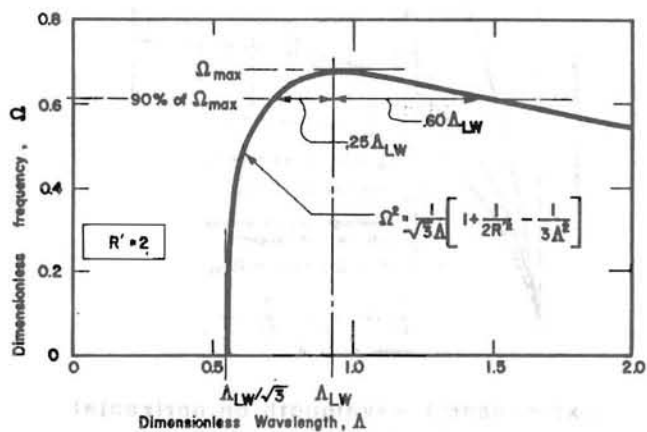
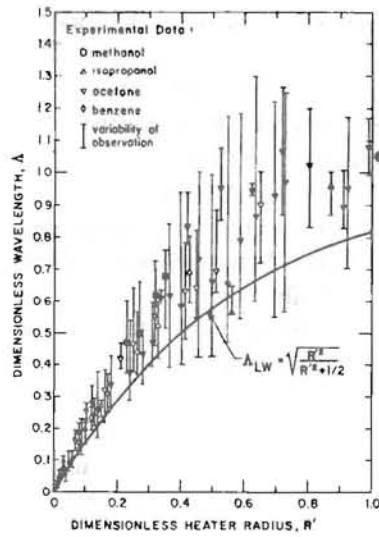
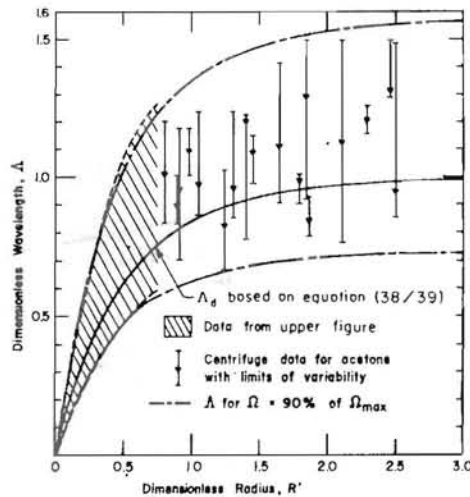


Fig. 21 The dimensionless form of Sun and Lienhard's /49/ dispersion relation (equation (37)) showing that a wide band of wavelengths around λ_D will yield close to the maximum frequency.



Experimental wavelength on horizontal cylindrical heaters – low R' range



Experimental wavelength on horizontal cylindrical heaters – high R' range

Fig. 22 Comparison of the 90-percent-of- Ω band of wavelengths with experimental film boiling data (from /49/) – showing short and long wavelength behavior.

The fact that both equation (43) and its Russian counterpart – devoid of any surface condition variables – correlated data for many fluids, all boiling in a similar geometry, gave strong support to the dimensional form (if not the theoretical basis) of the Zuber-Kutateladze q_{\max} equation.

In the years that followed it became clearer and clearer that geometrical shape and scale effects could not be ignored in the boiling transitions. The data sets used to test equation (43) were largely obtained on cylindrical heaters in size ranges for which q_{\max} , unfortunately, did not greatly differ from the flat plate value. But as more data accrued, they made it evident that these influences were important.

In 1964, Bobrovich et al. /53/ (and then, independently, Lienhard and Watanabe /54/) finally looked at the dimensional analysis of q_{\max} and q_{\min} . They noted that if q_{\max} depended on σ , $g(\rho_f - \rho_g)$, ρ_g , h_{fg} , and a characteristic length, L – 6 variables in the dimensions N, m, s, and J – then the dimensionless functional equations for q_{\max} and q_{\min} had to take the form

$$Ku = f(R') \quad (45)$$

where Zuber and Kutateladze had originally set $f(R')$ equal to a constant. Equation (45) was used in /53/ and /54/ to correlate data for horizontal cylinders. We illustrate such a correlation in the subsequent section.

The Prediction of Burnout on a Horizontal Cylinder. It was 1970 before Sun and Lienhard /55,56/ managed to make a hydrodynamic prediction of q_{\max} for another geometry – the horizontal cylinder configuration – and to set up the strategy by which subsequent predictions could also be made.

Figure 23, taken from the later work of Dhir and Lienhard /57/, shows how Sun modeled the vapor escape from a cylinder as a row of jets with radii of $(R + \delta)$. (The new parameter, δ – the vapor blanket thickness at the side of the cylinder – was a nuisance variable that had to be introduced to solve the problem.) A great deal of photographic evidence suggested that:

- the interface was messy enough to eliminate the action of transverse curvature observed by Lienhard and Wong;
- for small wires, jets were spaced on the Taylor “most dangerous” wavelength;
- that when $\lambda_d < 4(R + \delta)$, the jets would have to be spaced on $4(R + \delta)$ instead;
- that Zuber’s assumption that $\lambda_{H,c} = \lambda_{R,c} = 2\pi(R + \delta)$ was valid for the smaller cylinders;

- that, since λ_R becomes quite long above the larger cylinders, there is probably some shorter wavelength present to cause burnout;

and the most questionable of the assumptions,

- that $\lambda_H = \lambda_d$ for the larger configuration.

Sun and Lienhard argued that the jet is somehow “tuned” to the Taylor vibration in the horizontal interface around larger cylinders, and that it thus picks up this wavelength for λ_H . But the assumption is better supported by a simple dimensional argument:

We know from equations (28) and (26) that the burnout heat flux is inversely proportional to $\lambda_{H,c}$, and all the experimental data indicate that the

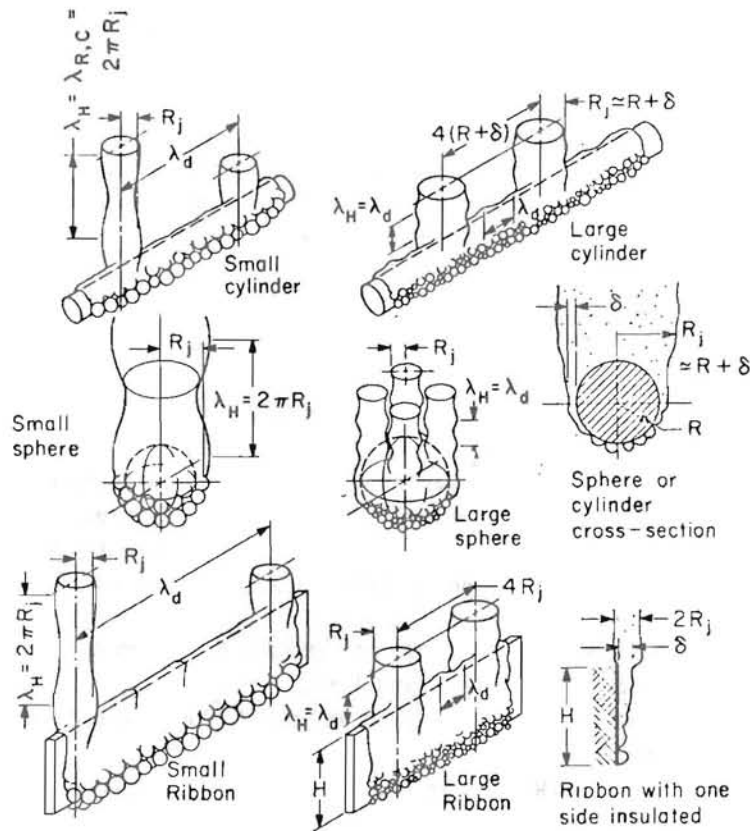


Fig. 23 Vapor removal configurations near the peak heat flux, on a variety of finite heaters /57/ or /63/.

influence of L' vanishes at large L' . Furthermore, photographic data show that the larger jet sizes increase in direct proportion to the heater size. But $\lambda_{R,c}$ is directly proportional to R . So if $\lambda_{R,c}$ defined the Helmholtz wavelength, the dimensionless peak heat flux would have to keep decreasing with R in large jets. It follows that we have to look for a Helmholtz wavelength that is independent of jet size. The Taylor wavelength is the only apparent measure that fits the requirement.

The q_{\max} derivation now follows simply. Combining equations (28), (26), and Zuber's q_{\max} , we obtain

$$\frac{Ku}{0.131} = \frac{q_{\max}}{q_{\max Z}} = \frac{24}{\pi} \sqrt{\frac{2\pi}{\lambda_H^3 g(\rho_f - \rho_g)/\sigma}} \frac{A_j}{A_n} \quad (46)$$

where $\lambda_H = \lambda_{R,c} = 2\pi R$ for small cylinders, and λ_d for large ones. The ratio A_j/A_h was obtained by simple mensurational calculation for the two geometries, and it included a variable, δ/R , which was obtained empirically from many photographs. The resulting heat flux prediction was

$$\frac{q_{\max}}{q_{\max Z}} = 0.89 + 2.27 \exp(-3.44\sqrt{R'}) \quad (47)$$

Equation (47) was compared with approximately 900 data points representing an enormous range of liquids, heater sizes, and gravity levels. The comparison is summarized in Fig. 24. For $R' > 0.15$, it represents the existing data within about ± 15 percent.

In 1972 Bakhru and Lienhard /58/ looked more closely at the left-hand side of Fig. 24. They did a Nukiyama-type of experiment and obtained boiling curves of the type shown in Fig. 25. Figure 25 is a typical boiling curve for a 0.0254mm platinum wire in saturated benzene. R' for this case is only 0.0076, which means that capillary forces completely outweigh buoyancy and inertia. Thus the hydrodynamic process vanishes completely and there no longer are any peak or minimum points.

It follows that, not only Sun's q_{\max} prediction but the entire hydrodynamic theory as well, ceases to be valid for $L' < \Theta(0.1)$.

4.5. The Dhir-Lienhard Predictions

Burnout on Submerged Bodies. Sun and Bakhru (and Ded, Rihard, and Keeling, whom we encounter subsequently) had been involved in the early

stages of a NASA-supported study of the influence of gravity that extended from 1967 to 1972 at the University of Kentucky. The work involved the use of a large centrifuge facility and the analysis of gravity influences in burnout. The last graduate student to work on that project, Vijay Dhir, made a remarkable set of extensions of prior work that firmly established the general validity of the hydrodynamic theory. Of course we still face unresolved issues within the theory, but after he finished, no reasonable person could doubt that these processes dominated the boiling transitions. Much of the work is summarized in /59/.

Taghavi-Tafreshi and Dhir's observation of frozen olive oil melting in warm water (made later on, in 1980 /60/) illustrates Dhir's instinct for illustrative experimentation and it gives a dramatic demonstration of the underlying Taylor wave behavior. A typical photograph, shown in Fig. 26, shows the square two-dimensional array of waves in a perfect analog to film boiling on a flat heater.

One of the first ^{of these} extensions of Zuber's theory was the revision of his flat plate prediction /61/. If we recognize that an infinite flat plate is a "large" configuration, and again use equations (26), (27, and (28), we must now replace $\lambda_{H,c}$ with λ_d . When we do this we obtain

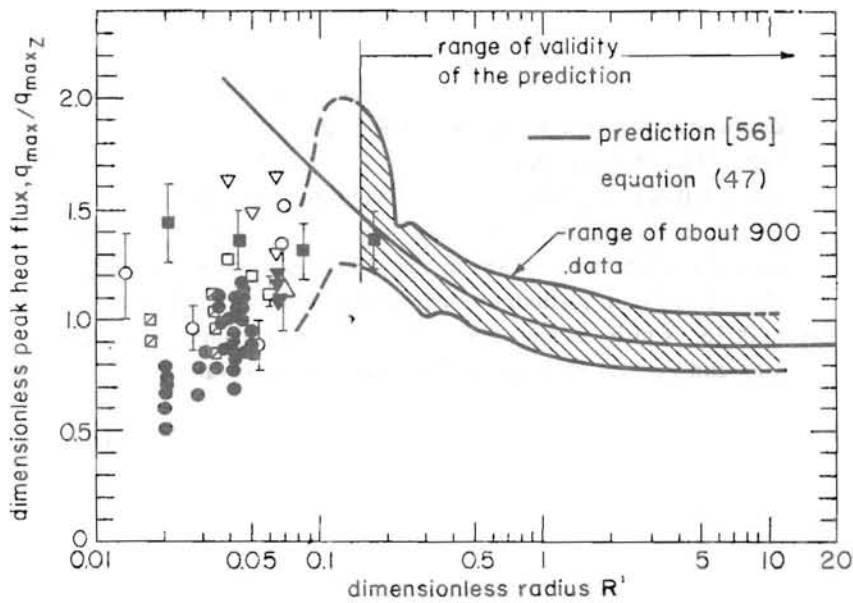


Fig. 24 Overview of the comparison of equation (47) with data.

$$Ku = 0.149 \text{ or } \frac{q_{\max}}{q_{\max Z}} = 1.14 \quad (47)$$

for the burnout prediction.

Equation (47) is compared with existing data in Fig. 27. There are two matters that need to be explained here:

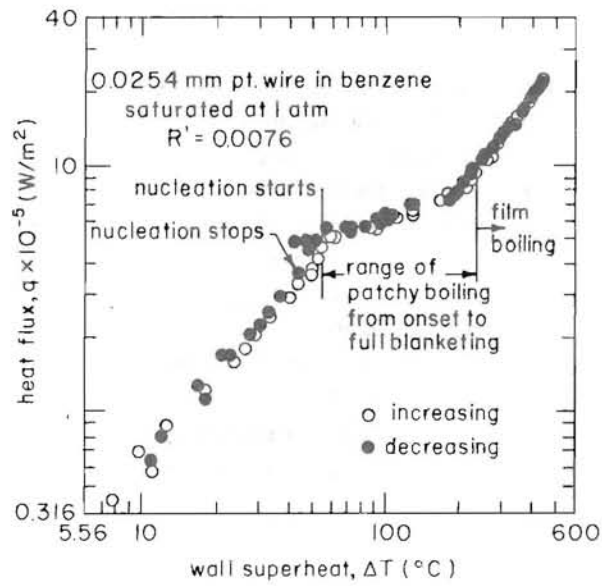


Fig. 25 Boiling curve for 0.0254 mm platinum wire in benzene /58/.

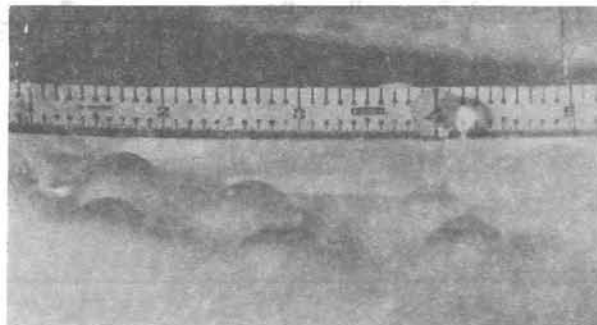


Fig. 26 Frozen olive oil melting below a pool of warm water /60/.

- Why, with all the boiling data that have been generated over the past 40 years, are there so few data here?
- What is wrong with the two data points (or with the theory) on the left side of the plot?

As to the matter of so few data: Most people who had measured burnout on flat plates failed to make the situation one-dimensional by protecting the vapor escape from induced side currents. These currents radically influence the peak heat flux. Only data obtained on flat heaters with vertical sidewalls along the edges can be used to approximate the infinite flat plate geometry.

The other matter – that of the variability of the data when the heater dimensions are on the order of the Taylor wavelength – is actually to be expected, according to the theory. When there are only one or two jets on the plate, the total peak heat transfer will stay constant while q_{max} drops, as the plate size is increased up to the point at which the plate is large enough to accommodate more jets. Thus q_{max} must display the sawtooth behavior shown in Fig. 28, with a steady decrease in q_{max} for any given number of jets on a plate, followed by a discontinuous rise in q_{max} each time new jets are added. Data from /61/ and one point given by Costello, Bock, and Nichols /62/ verify this behavior for small heaters.

The lone Costello et al. data point is particularly interesting because it was originally offered as evidence of the failure of the hydrodynamic theory. However, when we apply the theory with proper caution, this point supports it perfectly.

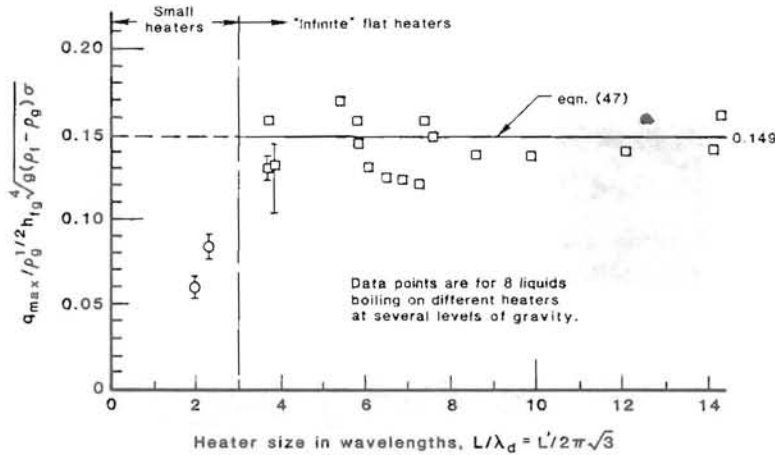


Fig. 27 Peak heat flux on broad flat heaters with vertical side walls.

These results also show that by compressing the heater area subtended by each jet, one may obtain as much as a two-fold enhancement of the burnout heat flux.

Dhir greatly expanded the valid flat plate data set by obtaining data in the centrifuge apparatus with a 6.35 mm diameter flat heater (with a vertical sidewall) subjected to as much as 17.5 times earth-normal gravity. The use of elevated gravity reduced λ_d to the point that the plate was as many as 14 wavelengths in diameter.

One might wonder why, if Zuber's theory underpredicts the configuration that it was meant to represent, was the failing so long undiscovered. The explanation is that it was constantly being compared to q_{max} in other geometries that yielded lower values. We turn to some of those predictions next.

Reference /57/ established the method by which predictions could be developed for a variety of submerged bodies. Dhir and Lienhard began with the general equation (46), and the assumed set of vapor removal configurations shown in Fig. 23. In each case they had to know how to specify $\lambda_{H,c}$, and the area ratio, A_j/A_h . They evaluated $\lambda_{H,c}$ as the Rayleigh wavelength for small heaters, and as the Taylor wavelength for large ones. A_j/A_h depends on L' , and on δ/R , which was usually evaluated by correlation of experimental data. In some cases this correlation of A_j/A_h was aided, and even replaced, by an

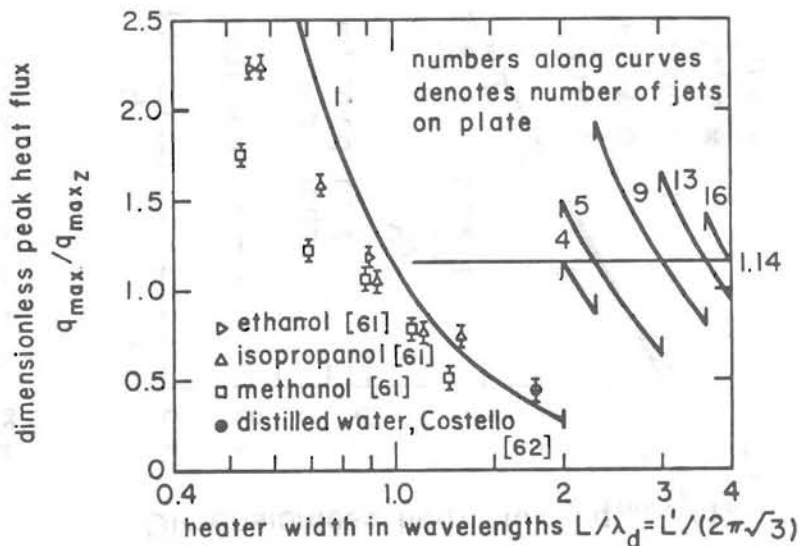


Fig. 28 Peak heat flux on a square finite flat plate with vertical side walls.

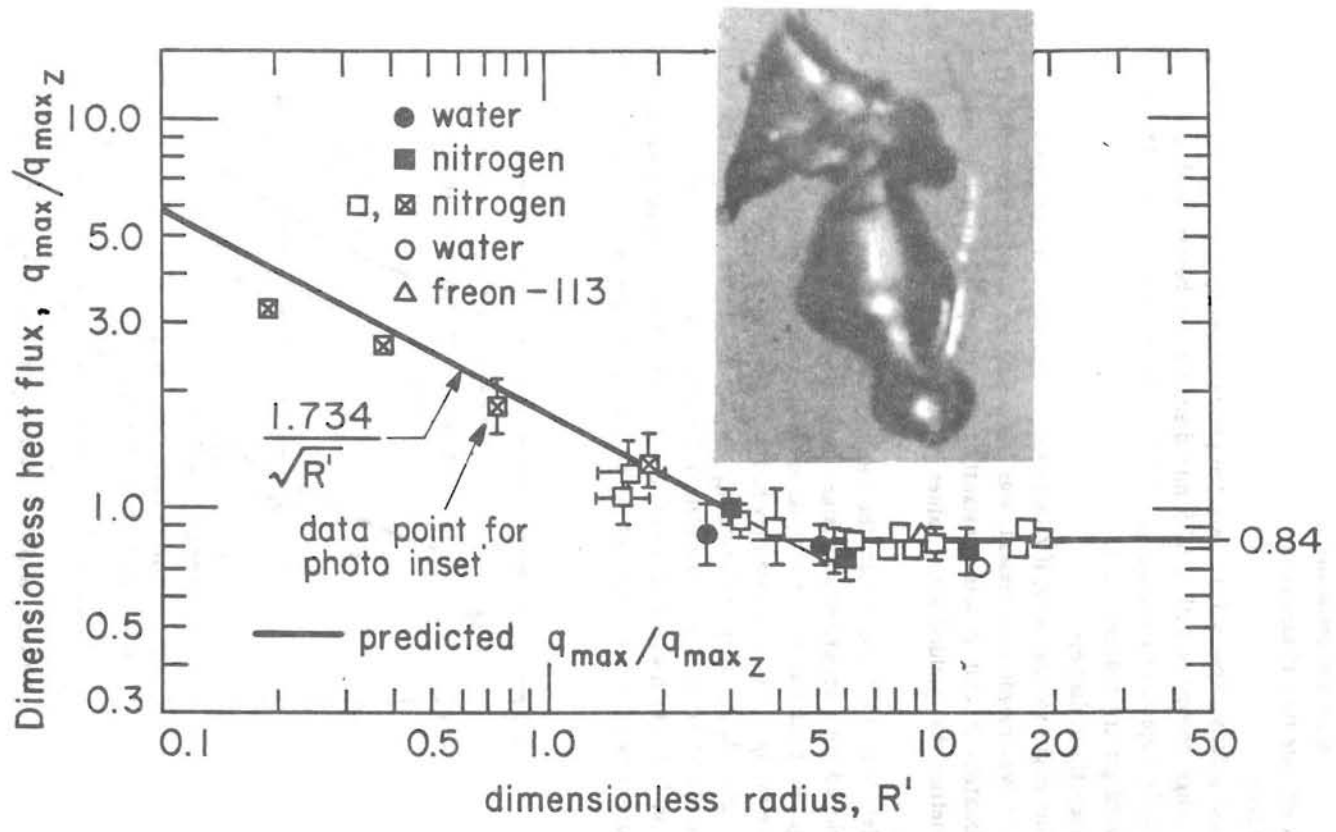


Fig. 29 q_{max} on spheres. Photo shows the vapor jet escaping from a 0.0795 cm dia. sphere in nitrogen ($R' = 0.75$).

elementary continuity argument that Ded /63/ had used in working out the case of the sphere.

Figure 29 compares these predictions for large and small spheres with data. The figure also includes a photograph of a small sphere which actually shows the collapsing Helmholtz-unstable, Rayleigh wave in the single escaping jet.

Figure 30 shows the collected predictions for the different geometries. Notice that $q_{max}/q_{max,Z}$ is equal to unity for the submerged cylinder data at L' (or R' in this case) just less than unity. Zuber's prediction was originally compared with cylinder data in this range and it fortuitously did quite well. It obviously does not predict burnout so well in other geometries — including the flat plate — or at other values of L' .

The Influence of Viscosity. We saw in Section 2.6 that Lewis, Taylor, and Bellman and Pennington had all recognized that viscosity could play a role in the hydrodynamic stabilities relevant to boiling. Yet not even the critics of the hydrodynamic theory showed much interest in the fact that Zuber's theory excludes the effects of viscosity. In the early 1970's Dhir went looking for this influence /64-66/.

He first turned his attention to the Taylor wave in film boiling /64,65/. Bellman and Pennington had extended the linearized stability theory to include viscosity. Dhir reconstructed their solution to include the transverse

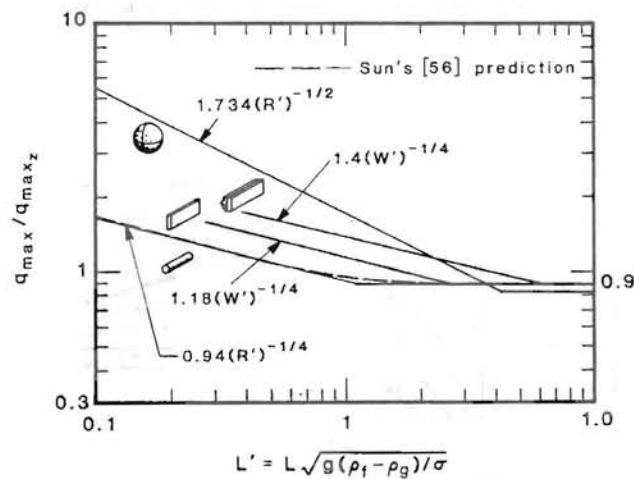


Fig. 30 Collected predictions of q_{max} for finite submerged heaters.

curvature term. The dispersion relation in this case takes the form of a four-by-four determinant of the coefficient matrix of the four equations of motion, which must vanish. He cast this in the form

$$\begin{aligned}
 & -2K + \frac{\Omega^2}{\Gamma K^2} + \frac{1}{(K^2 + \Omega M)^{1/2}} - \frac{K^2}{(K^2 + \Omega M)^{3/2}} - \\
 & - \frac{3K^2}{(K^2 + \Omega M)^{1/2}} + \frac{K^4}{(K^2 + \Omega M)^{3/2}} + \frac{\Omega^2 K}{\Gamma(K^2 + \Omega M)^{3/2}} \\
 & - \frac{4\Omega}{M\Gamma} + \frac{1}{2R'^2(K^2 + \Omega M)^{1/2}} - \frac{K^2}{2R'^2(K^2 + \Omega M)^{3/2}} = 0 \quad (48)
 \end{aligned}$$

where Ω is the previously defined dimensionless ω ; Γ , and K are

$$\Gamma \equiv (\rho_f - \rho_g)/(\rho_f + \rho_g) \quad \text{and} \quad K \equiv k[\sigma/g(\rho_f - \rho_g)]^{1/2} \quad (49)$$

and M is a newly defined viscosity parameter

$$M \equiv \frac{\rho_f \sigma^{3/4}}{\mu_f g^{1/4} (\rho_f - \rho_g)^{3/4}} \quad (50)$$

(which is close to being the square root of a Borishansky number).

This result is plotted for a flat plate in Fig. 31 (i.e., for $R' \rightarrow \infty$). Fig. 31 makes it clear that one may ignore viscosity when M is greater than 50. Additional results for various values of R' are given in /65/.

Dhir measured frequencies and wavelengths during low-heat-flux film

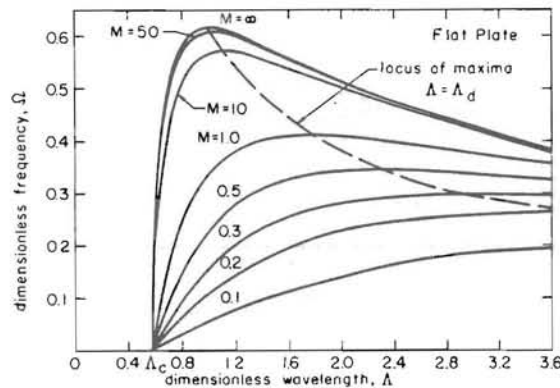


Fig. 31 Effect of viscosity on the dispersion relation for a flat plate.

boiling in cold (low-pressure) saturated cyclohexanol and obtained data that compare with equation (48) as shown in Fig. 32. (R'_c in Fig. 32 is R' based on $(R + \delta)$ for this configuration.) Figure 33 shows measured and predicted wavelengths for the smallest value of M that was observed. He also found that, at the upper limit of exponential growth (the limit of the linear theory), η/λ was on the order of 0.1 in this geometry. It appeared to decrease with increasing viscosity, while Lewis had found it to increase in his geometry. (No attempt has yet been made to investigate this limit systematically.)

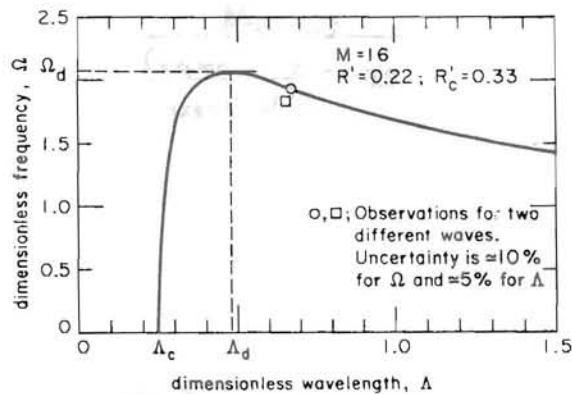


Fig. 32 Experimental verification of dispersion relation of cyclohexanol at 1.06 kPa. $q = 1.01(10)^5 \text{ W/m}^2$.

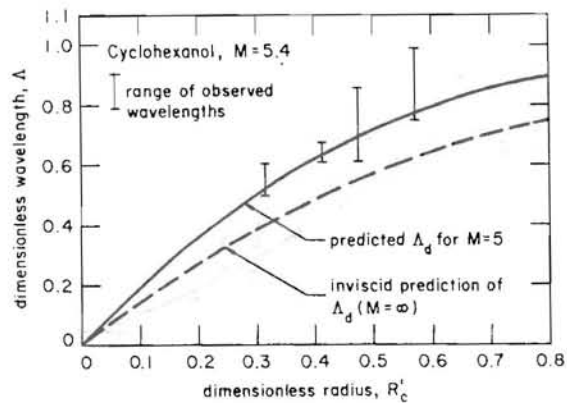


Fig. 33 Wavelengths on horizontal cylinders.

Although it was possible to discern the influence of viscosity in these experiments, the chief value of the work was to make it very clear that a liquid must be very viscous indeed before viscosity influences the Taylor process at all. For most real processes, it remains quite legitimate to ignore these influences.

Dhir also undertook the exceedingly complicated task of revising the Helmholtz stability arguments to include viscosity /66/. When the flat plate q_{\max} prediction was corrected using this $\lambda_{H,c}$ and the viscous λ_d , he obtained

$$\frac{q_{\max F}}{(q_{\max F})_{\text{inviscid}}} = \frac{0.264V/M\lambda_d^{1/2}}{\sqrt{1 - 0.0807 \left[\frac{V}{M^2\lambda_d} \frac{(q_{\max F})_{\text{inviscid}}}{q_{\max F}} \right]^{1/3}}} \quad (51)$$

where the constant 0.264 is empirical, $(q_{\max,F})_{\text{inviscid}}$ is the value predicted by equation (47), and V is a vapor viscosity parameter appropriate to this problem

$$V \equiv \frac{\sqrt{\rho_f \rho_g} \sigma^{3/4}}{\mu_g [g(\rho_f - \rho_g)]^{3/4}} \quad (52)$$

Equation (51) is compared with data for cold, saturated cyclohexanol in Fig. 34. Since these are earth-normal gravity data, the flat plate data here have been corrected for the effect of a finite number of jets on the heater. The cylinder data are included because they lie in the range of R' for which

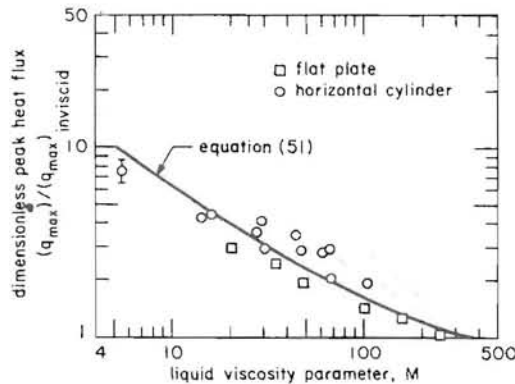


Fig. 34 Effect of liquid viscosity on peak heat flux for both flat plates and cylinders in cyclohexanol at earth-normal gravity.

q_{\max} is roughly the same on both flat plates and horizontal cylinders.

Figure 34 makes a very important fact clear, namely that high viscosity can greatly enhance the burnout heat flux – by as much as an order of magnitude.

By 1973 the hydrodynamic theory had gained widespread acceptance, and this new set of extensions was received without opposition. Still, problems still lurked in the use of the theory. For one thing the various q_{\min} predictions could never quite be made to work consistently. For another, Chang's and Costello's warnings that q_{\max} was not free from surface influences, and that in certain cases these influences could be magnified, remained valid. But these questions were laid aside for another decade.

The next order of business was that of attempting to extend the theory to flow boiling configurations.

5. The Hydrodynamic Theory of Flow Boiling

5.1. Induced Convection

The imposition of a convective flow on a boiling configuration radically alters the vapor removal structure. Imposed convection can range from almost inescapable induced convection effects to the imposition of high velocity flows. We begin by looking at induced convection.

When boiling occurs on an open plate in a liquid bath, the rising vapor entrains a pretty substantial flow of liquid into the vapor escape path. No one has really looked at this whole problem systematically, so we cannot predict its effect. However, we *can* show that induced convection can have a large influence on q_{\max} .

Costello et al. /62/ suggested in 1965 that induced convection might influence burnout. Five years later, Lienhard and Keeling /67/ looked at this problem systematically in the configuration shown Fig. 35. This experiment was done in a centrifuge, so it was possible to vary: gravity; the plate width, W ; and the boiled liquid. The smoothed data through upwards of a thousand data points are shown in Fig. 36.

The resulting burnout heat fluxes are normalized by Zuber's q_{\max} value, and plotted as a function of the two dimensionless parameters that are required by dimensional analysis:

- One parameter, N , is called the Borishanski number.

$$N \equiv \frac{\rho_f \sigma}{\mu_f^2} [g(\rho_f - \rho_g)]^{1/2} \quad (53)$$

It characterizes the variable of liquid viscosity which gives rise to the drag forces exerted by the rising bubbles.

- The other parameter is W' – an L' based on the heater width.

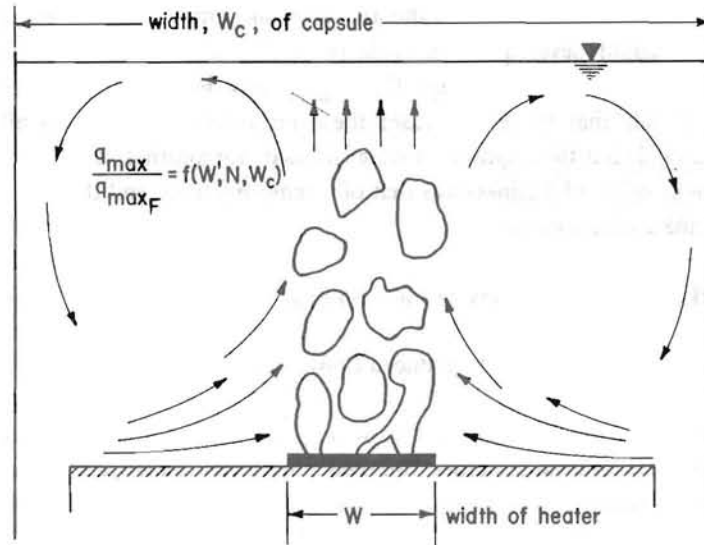


Fig. 35 End view of Keeling's ribbon heater configuration.

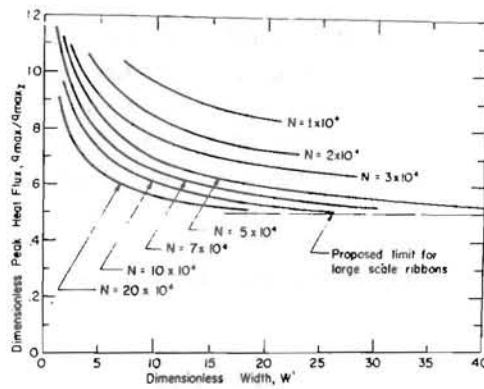


Fig. 36 The influence of induced convection from horizontal heaters.

We see that, at least in this particular configuration, induced convection normally has the influence of reducing the burnout heat flux to as little as half of $q_{\max,Z}$ — less than half of the regular flat plate value. But under the right conditions — large viscosity, small heaters, etc. — it can act the other way and actually increase the peak heat flux.

This result is illustrative, not general. It uses Keeling's container configuration to show that induced convection can have a dramatic influence on q_{\max} . Of course, the flat plate situation is one of the worst cases. Such submerged bodies as cylinders and spheres entrain some flow from below. But the flow is *parallel* with the vapor escape path. In these cases, the flow normally has a much smaller effect on the vapor escape process.

Still, we have made unpublished observations which show that serious influences of induced convection are possible, even in such geometries. E.K. Ungar recently tried to make a pool boiling q_{\max} measurement on a horizontal cylinder in the test section of a vertical flow loop in our Heat Transfer/Phase Change Laboratory. The loop acted like a thermo-syphon and noticeably augmented the induced flow. Preliminary results showed about a 20 percent drop in q_{\max} when he opened the system to the atmosphere and interrupted the induced convection action.

5.2. Burnout During Crossflow over a Horizontal Cylinder

Burnout on horizontal cylinders subject to a liquid crossflow has received attention since shortly after WW-II. In this configuration, an almost two-dimensional vapor sheet leaves the cylinder (see Fig. 37) for all but very slow flows. The first highly controlled measurements, accompanied with very good photographic visualizations, and relatively free of such system problems, were those of Vliet and Leppert in 1964 /68,69/. Cochran and Andracchio /70/ measured burnout in both water and Freon-113 in 1974, and in 1975 Min /71/ observed burnout in methanol as well.

The first q_{\max} prediction for this arrangement was made by Lienhard and Eichhorn /72/ in 1976. The problem that they faced was that, although this appeared to be a straightforward Helmholtz instability problem, the Helmholtz wavelength in the sheet was not known and it clearly varied in some unknown way with the system parameters.

They got around this by recasting the conventional minimum energy definition of mechanical stability into what they called a Mechanical Energy Stability Criterion, or "MESc." They argued that, since there were no heat transfer processes in the vapor wake, the net input of mechanical energy to the wake had to be less than the net rate of energy consumption. This global

criterion had the advantage of predicting burnout without requiring full details of the instability mechanism that actually gave rise to burnout. Its disadvantage was that it required knowledge of the vapor sheet thickness, αD , which had to be evaluated semi-empirically.

Three years later, Lienhard and Hasan /73/ used the MESC to rederive q_{\max} for certain pool boiling configurations. We shall not review this work here except to note that, since the MESC must necessarily embrace the Helmholtz instability, they actually had to replace their uncertainty of one aspect of the vapor escape process with an uncertainty about a different aspect of it. They removed the need for assuming $\lambda_{H,c}$, and replaced it with the need for a knowledge of the bubble departure diameter (which they generalized from a large number of photos of boiling).

The 1976 q_{\max} prediction was followed by two stages of improvement. In 1981, Hasan et al. /74/ ran higher speed experiments which made it clear that most of the previous data had been subject to the influence of gravity – a system parameter that did not appear in the previous prediction. They accordingly rebuilt the correlation based only on gravity-free data. Then in 1985, Kheyrandish and Lienhard /75/ discovered an incorrect assumption in

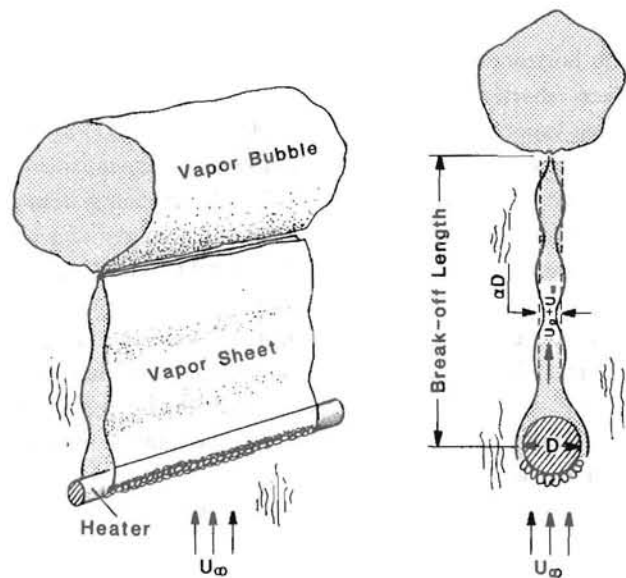


Fig. 37 Vapor removal configuration near burnout during cross-flow on a horizontal cylinder.

/72/ and /74/, and they again emended the prediction. We shall briefly review the prediction in /75/, indicating how the earlier works were altered.

We begin by placing a control volume (C.V.), that moves *with the liquid*, around the vapor wake, as shown in Fig. 38. The cylinder moves away from the C.V. at the speed of the liquid, u_∞ , and the line along which the bubbles break away moves downward, in steps, within the C.V.. The average downward speed of the breakoff line is also equal to u_∞ . The bubbles left behind remain stationary in the liquid when gravity can be ignored.

Next, we apply the MESC. To do this, we equate the rate of flow of kinetic energy into the C.V., to the rate at which surface energy is consumed in the C.V. (The reason that we speak of surface energy consumption is that the length of the sheet is actually shrinking *within the C.V.* as bubbles are nipped off.) The MESC tells us that the vapor escape path will be unstable if the rate of surface energy consumption within the C.V. (less the surface energy left behind in the large bubbles) exceeds the rate of supply of kinetic energy. Therefore we equate these two rates and obtain

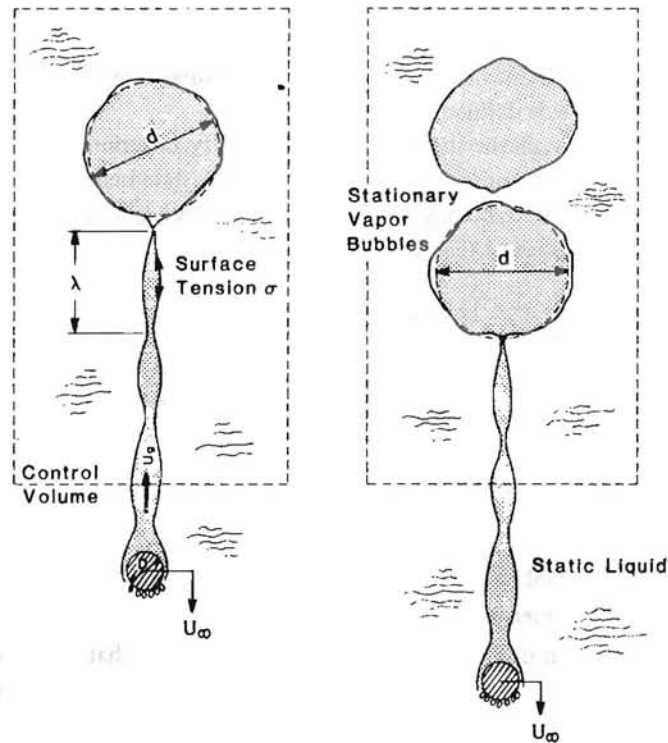


Fig. 38 Control volume for the MESC formulation.

$$\frac{1}{2}\rho_g \alpha (2R) u_g^3 - 2u_\infty \sigma + \pi d \sigma / \tau = 0 \quad (54)$$

where d is the diameter of the escaping two-dimensional bubble (see Fig. 38), and the term, τ , is the period of bubble breakoff. Notice that the left side of equation (54) is less than zero in the nucleate boiling regime and reaches zero at burnout. In this calculation, the kinetic energy flux of liquid leaving the sides of the C.V. is neglected since widening the C.V. will make it as low as we wish without adding any surface area to the sides.

Continuity requires: $\pi d^2/4 = \alpha (2R) u_g \tau$, which we solve for d .

$$d = 2\sqrt{\alpha \tau (2R) u_g / \pi} \quad (55)$$

Substituting equation (55) in (54) we obtain

$$\frac{u_g}{u_\infty} = \left(\frac{4}{\alpha We}\right)^{1/3} \left[1 - \sqrt{\pi \left(\frac{2\alpha R}{u_\infty \tau}\right) \left(\frac{u_g}{u_\infty}\right)}\right]^{1/3} \quad (56)$$

where the group $2R/u_\infty \tau$ is identifiable as a Strouhal number, St , and the Weber number, We , is defined as $2\rho_g u_\infty^2 / \sigma$.

Equation (55) replaces the Helmholtz instability criterion for the vapor velocity, u_g . Next we need an energy conservation statement, equivalent to equation (28), for flow boiling. In this case the energy balance between the heat flux at the surface of the cylinder and the escaping vapor yields

$$\phi \equiv \frac{\pi q_{\max}}{\rho_g h_{fg} u_\infty} = \alpha [1 + u_g / u_\infty] \quad (57)$$

where the term, 1; on the right side adds u_∞ to u_g since u_g is relative to the liquid and we need a velocity relative to the moving cylinder.

Substituting equation (56) in (57) gives the q_{\max} prediction

$$(\phi - \alpha)^3 \equiv (4\alpha^2 / We) [1 - \sqrt{(\pi St) \gamma}] \quad (58)$$

Equation (58) is implicit in the dependent variable, ϕ ; however, that creates only minor inconvenience in solving it.

This formulation differs from the original one /72/ in that it includes the capillary energy left behind in the bubbles, represented by the term $\pi d \sigma / \tau$ in equation (54). Without a knowledge of τ , there originally seemed to be insufficient information to evaluate this contribution, and it (erroneously) seemed reasonable to Lienhard and Eichhorn to ignore it.

Kheyrandish and Lienhard's observations of the wake showed the existing data represented two situations: when small wires were heated by alternating current, the wake responded to the resulting 120 Hertz oscillation in the heat input. When the cylinder was heated with a steady power supply it did not. Thus different strategies are needed to predict a.c. and non-a.c. burnout.

These observations also showed that, near q_{max} , there are constantly collapsing waves in the walls of the vapor sheet. The length of these waves increases with q , up to $u_{\infty}/120$ at burnout. The clear implication is that these waves *travel* toward the cylinder until burnout, at which time they grow in place in the liquid, as true Helmholtz unstable waves.

Hasan et al. [74] provided experimental data of the kind shown in Fig. 39, where we see q_{max} as a function of u_{∞} for both upflows (u_{∞} = positive) and downflows (u_{∞} = negative). For large values of $|u_{\infty}|$ the velocity dependence of q_{max} is identical in either direction — hence it is gravity-independent. For slower flows, particularly slow downflows which can suspend a bubble about the wire, q_{max} can be strongly gravity-dependent.

Hasan et al. developed a "gravity influence parameter", G , which, when it was ≥ 10 , assured gravity independence:

$$G \equiv u_{\infty}/(g\sigma/\rho_f)^{1/4} \geq 10 \tag{59}$$

Everything that follows is based on data for which $G \geq 10$.

The next problem is that of determining α . Since the liquid flow is "lubricated" by the vapor flow everywhere but in a 90° or so arc about the

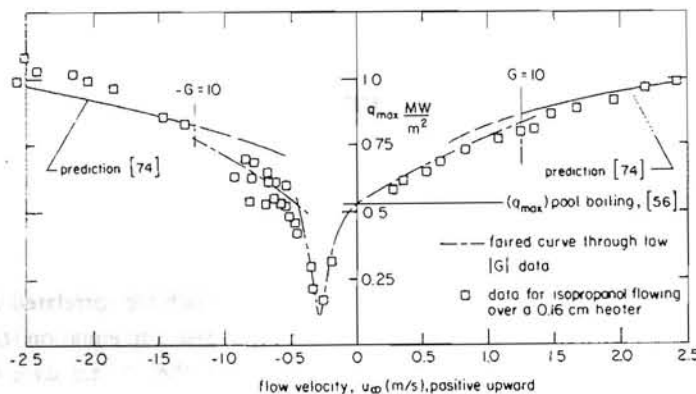


Fig. 39 Typical influence of liquid velocity on q_{max} for horizontal cylinders.

stagnation point, we expect a nearly "potential" flow in the liquid. Yet no one has managed to make an *a priori* prediction of α . Recently Kheyrandish and Dalton /76/ made a potential flow calculation that gave the shape of the wake; but they had to use data, in a different way than we have here, to get α .

For the a.c. data, we can generate a set of α values by substituting data in equation (58) and using the known Strouhal Number for a.c., $120D/u_\infty$. These α 's are correlated within an rms scatter of ± 6 percent by

$$\alpha = 0.002r^{7/8}/We^{0.15} \quad (60)$$

where $r \equiv \rho_l/\rho_g$.

Substituting equation (60) into (58) we obtain

$$\frac{(\phi - \alpha)}{[1 - \sqrt{\pi St(\phi - \alpha)}]^{1/3}} = 0.0252r^{0.583}/We^{0.43} \quad (61)$$

Equation (61) is compared with the existing a.c. data in Fig. 40. The results correlate within an rms scatter of ± 8 percent on the coordinates required by equation (58).

For non-a.c. data we need an additional piece of information to eliminate one of the two unknowns τ and α . For that we go to Haggerty and Shea /33/ who analyzed the stability of a thin vapor sheet such as we have here. Their results can be put in the following form to give the most rapidly collapsing Helmholtz wavelength, $\lambda_{H,d}$:

$$\frac{\lambda_{H,d}}{D} = \frac{2\pi}{u_g/u_\infty} \sqrt{\frac{3\alpha}{2We}} \quad (62)$$

Combining equations (58), (62), and (56) we obtain

$$\frac{(\phi - \alpha)}{[1 - \sqrt{\pi St(\phi - \alpha)}]^{1/3}} = 0.051r^{0.526}/We^{0.39} \quad (63)$$

We once more use data to create a set of α values which are correlated within ± 7 percent by $\alpha = 0.0058r^{0.79}/We^{0.085}$. Using this result in equation (63) we get the correlation shown in Fig. 40. This represents the non-a.c. data within an rms scatter of ± 4 percent.

Figure 40 includes five Broussard, Yilmaz, and Westwater /77,78/ data on

the left side which are identified as being cases for which $\lambda_{H,d}/2R < 1$. Since the present theory is based on a sheet leaving the cylinder, and since a sheet cannot develop when the wavelength becomes short enough, it is unlikely that the present theory represents these data.

5.3. Burnout in the Jet Disc Configuration

No other application of the hydrodynamic theory has been made to a submerged flow-boiling burnout configuration. However, a good deal of work has been done on the jet-disc arrangement shown in Fig. 41. This can take different forms: a circular jet on a round disc heater, a slit jet on a square heater, various angled or off-center jets, arrays of jets, etc..

The basic experimental work on this system has almost all been done by Katto and his co-workers [79-83]. They have reached *very* high cooling rates with it — as high as 18.26 MW/m² in water.

Notice what happens to the liquid flow (Fig. 41). Part of it moves along

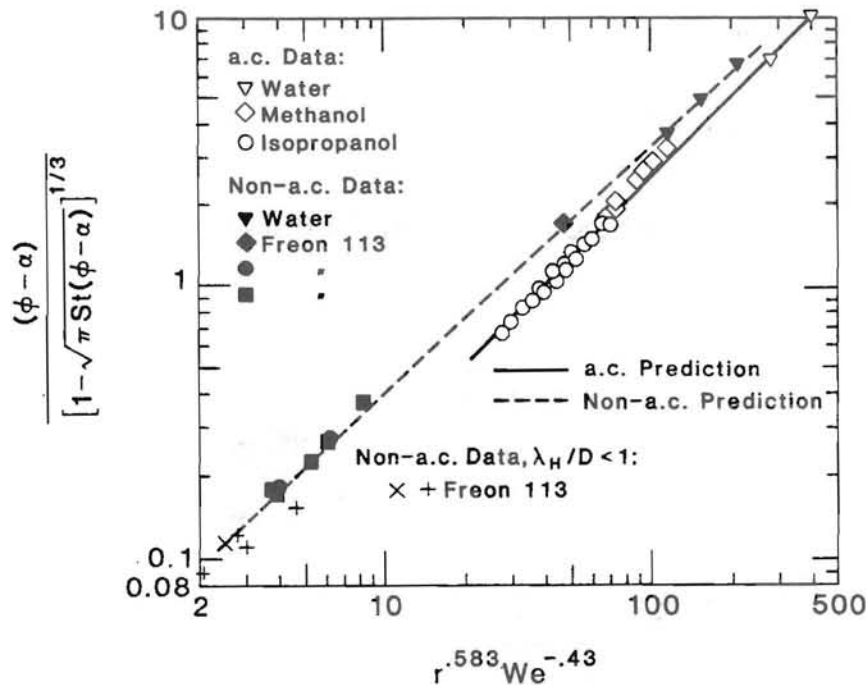


Fig. 40 Correlation of both a.c. and d.c. burnout data in the coordinates required by MESIC formulation.

the plate, being perforated by bubbles as it goes. The other part is a fairly fine spray of liquid droplets, flung upward and outward at a somewhat flat angle with the plate.

The prediction of burnout in this configuration was undertaken analytically by Lienhard and Eichhorn /84/ in 1979 in what was the second application of the MESC to a flow boiling problem. Like the cylinder burnout solution, this was subsequently reworked with the aid of new information in 1985 /85/. We shall briefly review the latter formulation.

In this situation we calculate the rate at which vapor kinetic energy flows up from the plate and equate it to the rate that surface energy is created in forming the droplet spray. Burnout must then occur when the kinetic energy flows into the wake structure faster than new surface energy can absorb it. We call the fraction of the liquid converted into spray, α , the jet and disc diameters, d and D , and an appropriate mean droplet diameter, δ , and we get

$$v_g(\pi D^2/4) \frac{\rho_g v_g^2}{2} = \alpha \frac{\rho_f u_\infty (\pi/4) d^2}{\rho_f (\pi/6) \delta^3} \pi \delta^2 \sigma \tag{64}$$

which reduces to

$$\phi = \alpha^{1/3} \frac{(d/\delta)^{1/3} r^{1/3}}{(\beta We)^{1/3}} \tag{65}$$

where $\phi \equiv q_{max}/\rho_g h_{fg} u_\infty$, $We \equiv \rho_f u_f^2 D/\sigma$, $\beta \equiv d/D$, and $r \equiv \rho_f/\rho_g$.

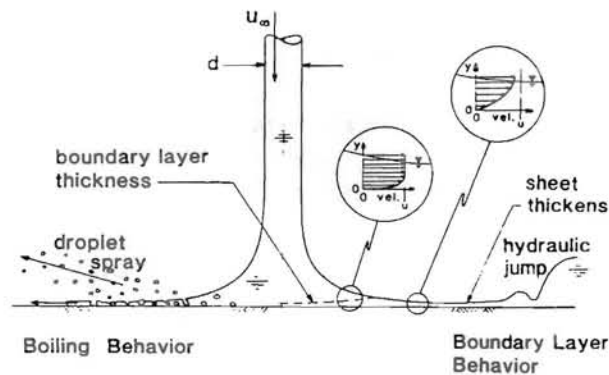


Fig. 41 The jet-disc boiling heat removal configuration.

The problem with equation (65) is that it brings the unknown average droplet diameter, δ , into the result. (There always seems to be one unknown in these problems. Previously, it was a Helmholtz wavelength or a departing bubble size, and now it is a droplet diameter.) To get around this, Lienhard and Eichhorn /84/ used the classical Nukayama-Tanasawa /86/ droplet formation equation to infer a dimensionless expression for d/δ in terms of We , ϕ , and β . Based on careful dimensional arguments, Sharan and Lienhard /85/ revised this expression into the form

$$(d/\delta) = f(r)We^{1/6} \quad (66)$$

Using additional experimental evidence, they assumed that $\alpha = (a \text{ function of } r) We^a$, where a is an empirical constant, so substituting equation (66) in (65), they obtained

$$\phi\beta^{1/3} = f(r)[1000/We]^A(r) \quad (67)$$

where A is a modified constant that, they noted, might depend on r .

Although equation (67) contains two undetermined functions of r , it is otherwise an exceedingly restrictive function of its three dimensionless variables — the MESC has therefore provided a great deal of information. To eliminate the functions, the data of Katto, Monde, and Shimizu /80,82/ are plotted on $\phi\beta^{1/3}$ vs. We coordinates as shown in Fig. 42, for three fluids at different pressures — each case representing a different value of r . The following functions are faired through the resulting values of $f(r)$ and $A(r)$.

$$f(r) = 0.21 + 0.00171r \quad (68)$$

and

$$A(r) = 0.486 + 0.06052 \ln r - 0.0378(\ln r)^2 + 0.00362(\ln r)^3 \quad (69)$$

Equation (67) with equations (68) and (69) is plotted against the data in Fig. 43. It represents the data within an rms error of only 8.7 percent. Sharan and Lienhard also analyzed the influences of gravity and viscosity in this problem. They showed that it was legitimate to neglect these influences when

$$\beta/Re^{1/3} < 0.40 \text{ and } u/\sqrt{gD} \geq 8 \quad (70)$$

All data that violated these criteria were eliminated from the data correlations.

Thus far, the cylinder in a cross-flow, the jet-disc configuration, and several pool boiling configurations are all of the situations that have been treated with the Mechanical Energy Stability Criterion. The question that remains is, "What other problems might it eventually solve?" We would certainly hope that it might eventually find application to additional ones including the important and elusive problem of burnout in a pipe.

6. The Transition Boiling Region Revisited

6.1. The View of the Transition Boiling Region in 1980

The focus of work on the Hydrodynamic Theory during the years between 1961 (Berenson) and 1980 was not on the transition region. Nevertheless, the literature of that period reflected a growing uneasiness with our understanding of the region.

The Vapor Explosion Problem. Much of this uneasiness was stimulated by the need to understand non-chemical explosions that plagued many

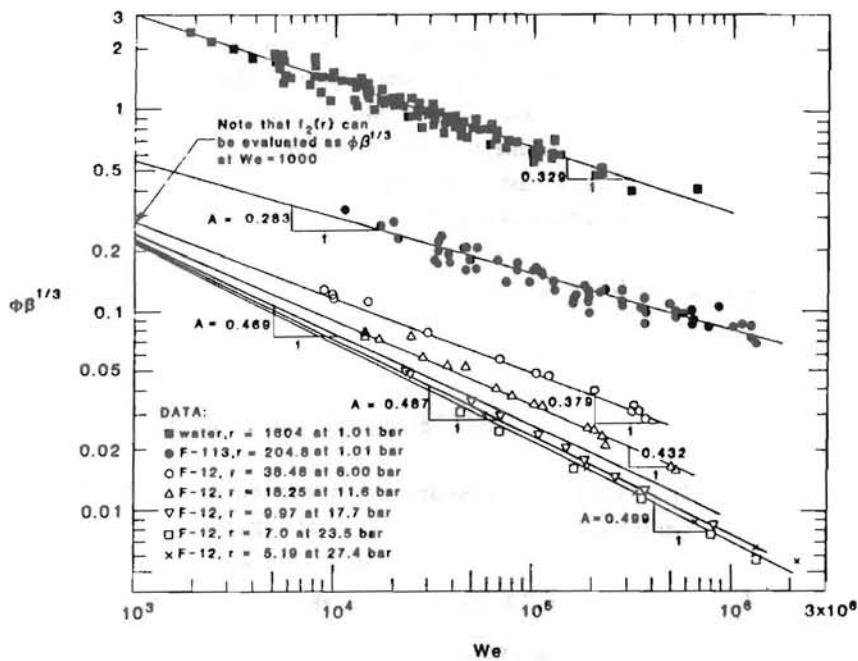


Fig. 42 Experimental determination of values of $f(r)$ and $A(r)$.

industries in which hot molten materials could accidentally contact cooling liquids. Metal refineries and foundries, and paper pulp plants as well, had suffered such explosions for decades; but little had been found out about what caused them. Serious loss of property, life, and limb were common occurrences in the metals industry (see Witte and Cox /87/). Such incidents became known as vapor explosions, reflecting the conversion of thermal energy into mechanical energy by the production of vapor in the extremely rapid boiling processes.

Morison /88/ wrote of the development of the Bessemer iron-to-steel conversion process in the 1860's, saying:

“Once a careless worker poured two tons of molten metal into a chilling pit at Wyandotte (Pennsylvania) in which there were only a few gallons of water. The resulting explosion hurled a United States senator, who had come to observe the new miracle, across the room and blew Eber Ward [the developer of the process] out the door and on to a scrap pile.”

Neither Eber Ward nor the senator were seriously injured, so Ward's efforts at

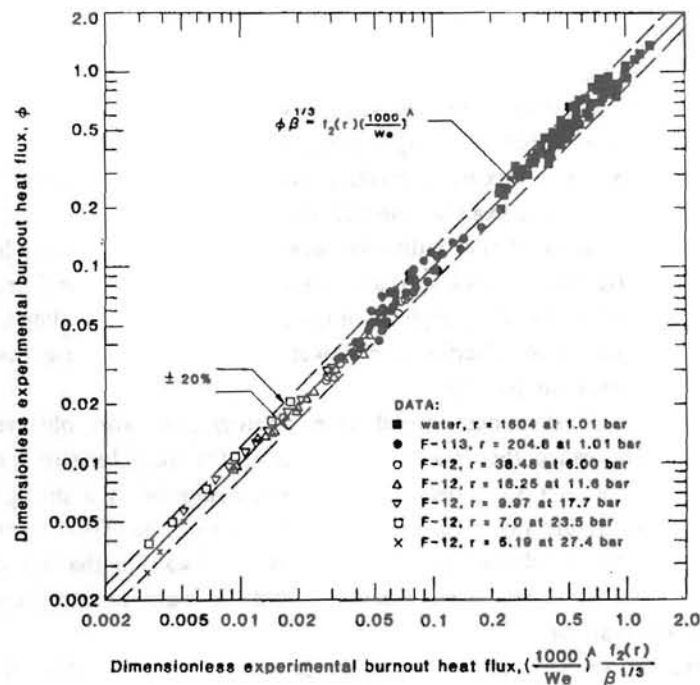


Fig. 43 Comparison of q_{max} correlation for jet-disc burnout, with data.

public relations came to a comical end; however, the threat of explosive vapor production lingers even now.

The possibility of vapor explosions began to threaten the safety of nuclear power reactors in the mid-1960's, and it had the side effect of renewing interest in the transition boiling regime. The SPERT reactor test program /89/ was intentionally designed to subject test reactors to severe operating conditions. In 1963 the SPERT 1-D reactor unexpectedly suffered a vapor explosive when it was subjected to a severe overpower nuclear transient. Pressure transducers recorded a pulse in excess of 200 atmospheres that destroyed the reactor. Subsequent analysis of the record showed that a portion of the core had melted and come into contact with the reactor cooling water.

The nuclear industry carried out extensive investigations of the vapor explosion phenomenon — which they called the “fuel-coolant interaction” — between the mid-1960's and the late 1970's. This massive research program showed that such explosions are triggered by contact of the coolant with molten core material. When the superheated liquid flashes, the resulting hydrodynamic action fragments the molten material, increasing its surface area, thus leading to a propagation of the explosion.

Indeed there was heavy controversy during this period as to why heat transfer to the surrounding coolant was so rapid. For the sake of brevity we do not trace that spirited controversy. However, the important concept that came out of it was that an abrupt change from film to transition boiling initiated the explosive mixing of molten metal and a volatile coolant. This forced investigators to re-examine the transition boiling region.

Consequently some of the traditional ideas about transition boiling began to tumble. Witte and co-workers (data reported in /90/) reported jumps in heat transfer in the transition regime for quenched bodies. Subcooling of the liquid exacerbated such behavior — the lower the liquid temperature was, the more dramatic such jumps were.

Stevens /91/, using high speed cine photography, also observed a phenomenon he called the “transplosion” during the quenching of spheres being forced through subcooled water. The transplosion is a precipitous collapse of the stable vapor film into the transition regime. The fascinating thing about these transitions is that there is no visual warning that the vapor film is about to collapse — no observable unstable wave structure on the interface, for example.

Stevens also showed that the transition regime is not just a mixture of film boiling and nucleate boiling, rather it has a hydrodynamic structure of its own which in some cases bears a resemblance to film boiling and in others

looks much like nucleate boiling. Furthermore the photographs provided compelling evidence that liquid-solid contact occurs not only in the transition regime but in the stable film boiling regime as well, as the minimum heat flux is approached. In 1966 Bradfield /92/ had measured liquid-solid contact in what appeared to be the stable film boiling regime. He found that surface roughness and liquid temperature were quite important in determining whether such contacts might occur.

The meaning of this behavior becomes clearer in Fig. 44 where we illustrate the portion of the film boiling curve near q_{\min} . While the slope of the q - ΔT curve is still positive, we now know that substantial liquid-solid contacts can occur. We henceforth refer to this as part of the "transition-film boiling" region. Although it wasn't clear at the time, we now know that, depending upon the extent of wetting that the contacts entail, the q - ΔT curve can depart substantially from the curve that represents film boiling without any liquid contact.

Henry /93/, in 1974, reported that liquid-liquid boiling surfaces were prone to such contacts as well. At about the same time, he /94/ had modified Berenson's q_{\min} prediction to include the effects of liquid-solid contacts as the vapor escapes from the liquid-vapor interface. He enjoyed notable success in predicting the apparent minimum boiling temperature differences that had been measured by several investigators using quenching techniques.

The controversy over whether or not liquid-solid contact occurs in the transition region encouraged several investigators to measure such contacts. We have already mentioned Bradfield's pioneering work. In 1978, Yao and

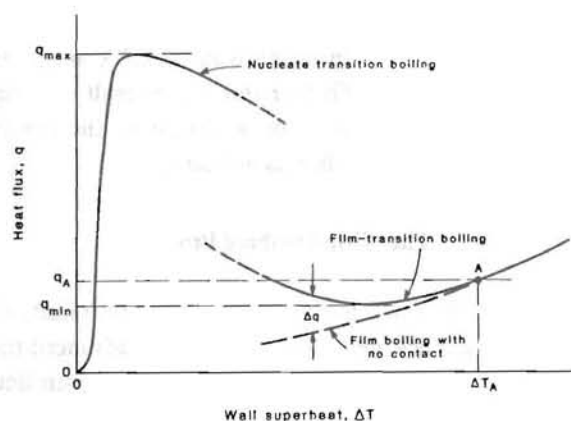


Fig. 44 Qualitative representation of the film-transition and nucleate-transition regions showing the effect of liquid-solid contact on the film-transition curve.

Henry /95/ used a conductance probe to measure liquid-solid contact during the film boiling of ethanol on various surfaces. Although their data were scattered, they showed that there is indeed liquid-solid contact in the transition-film boiling region including that portion in which a negative $q-\Delta T$ slope exists. Subsequently Ragheb and Cheng /96/, Lee et al. /97/, Swanson /98/ and Groendes and Mesler /99/ provided even more evidence that such contacts occur.

Inaccessibility of the Transition Regime. Stephan's realization /100,101/, in 1965, that access to the transition boiling curve is limited by resistance between the heat source and the boiling liquid also stimulated the re-examination of the conventional view of transition boiling. Kovalev /102/ and Grassmann and Zeigler /103/ verified Stephan's analysis soon after he proposed it (recall section 2.3).

Hesse /18/ used what was known about transition boiling stability in 1973 to design experiments in which almost all of the transition boiling curves for low pressure Freon 12 and 113 could be reached. However, he points out for Freon 12 at 30 bar:

“...the characteristic boiling curve in the transition region is steeper than the characteristic of the heating surface; consequently there are no stable operating points”.

The “characteristic” of the heating surface that Hesse refers to here is given by equation (2).

We re-emphasize that much of the transition zone might be inaccessible even for non-electrically heated systems. Hesse's results showed that an increasing fraction of the transition region is inaccessible at higher pressure, for a given heater configuration. Whether this is the result of a change in the slope of the transition boiling curve, or a change in the contribution of $R_{\text{condensation}}$ to the characteristic line, is not clear.

6.2. The Witte-Lienhard Proposal

Witte and Lienhard /90/ undertook a careful review of transition boiling in 1982 in the light of these new developments and they advanced the idea that there are two “transition” boiling curves accessible to a given liquid boiling on a given surface. A variety of saturated, subcooled, pool and flow boiling data were shown to be consistent with, and explainable in terms of, the idea.

The two curves in Fig. 44 are simply called *nucleate* and *film* boiling. As q

is increased, in the conventional nucleate boiling regime, to a value beyond q_{\max} , the collapse of the vapor escape path will be catastrophic. On the other hand, if ΔT is increased independently, the vapor removal pattern changes continuously, and the jets and columns mechanism will not disappear all at once.

There will instead be an increase in the number of nucleation sites and an increased tendency to separate the liquid from the surface, just beyond the peak of the curve. As the surface grows hotter, the duration of the liquid contact will be reduced. When liquid moves into the dry patch, heavy nucleation will tend to blow it away quickly, much as Zuber suggested (recall Fig. 12). The hydrodynamic jets and columns mechanism is still admissible because the vapor production is below the critical value, but the disruptive situation at the surface leads more and more to oscillating liquid contact — to batchwise “explosions” of vapor into the liquid bulk.

The film boiling curve is also extended (to the left) beyond the point, A, where contact causes it to depart by an increment, Δq , in heat flux from the pure film boiling curve. This deviation increases more rapidly than the pure film boiling heat flux drop, as ΔT is reduced, defining a local minimum in the heat flux. We still designate this minimum flux as q_{\min} although it is no longer Zuber’s hydrodynamic minimum. (The possibility of contact to the right of q_{\min} was not discussed in /90/; that came later.)

In 1982 we opted to drop the term transition boiling; rather we suggest that the region ought to be viewed as an extension of either film boiling or nucleate boiling. Drew and Mueller /9/ simply identified the region as a part of the film boiling region and did not use the word “transition”. Later such terms as “partial” or “unstable” film boiling were introduced, and then dropped in favor of the term “transition” which did not commit anyone to a hypothetical mechanism. For the sake of clarity, we now speak of “nucleate-transition” and “film-transition” boiling to distinguish the two curves.

Winterton /104/, in a discussion of the Witte-Lienhard concept, suggested that there are a multitude of curves that a given heater and liquid combination might follow in the “transition” region, depending upon the wetting nature, as characterized by the contact angle, of the liquid upon contact with the heater. This is not at odds with our proposal. We assume that a system will “choose” either the possible nucleate-transition or the film transition curves at a given ΔT . By controlling the wetting characteristics of the system, one could create a multitude of curves for a given liquid-heater combination.

The jumps in heat transfer and the transplosion phenomenon alluded to in

Section 6.1 can readily be explained by the two-curve transition concept. Some of Berenson's data which showed dramatic shifts in heat flux when wetting agents were added to the boiling liquids also fit the hypothesis quite well. Ungar and Eichhorn /105/ and Sankaran and Witte /106/ also observed such jumps in heat transfer for copper spheres cooling in stationary and flowing liquids.

Observations reported in /90/ suggest that, in quenching situations, the system follows the nucleate-transition curve when the hydrodynamics of film boiling permit liquid-solid contact so liquid can spread upon the surface and allow nucleation to occur. If the contacts are fleeting because the liquid does not spread, no nucleation occurs and the system follows the film-transition curve. Take mercury as an example; it is well-known that for surfaces not wet by mercury, no nucleate boiling occurs anywhere. As ΔT is increased, the system goes over to film boiling rather than through the conventional isolated bubbles, jets and columns, q_{\max} , and transition regions.

6.3. Recent Findings

If we take the view that there are two continuous transition regions — nucleate-transition and film-transition — then we are immediately challenged to ask what happens when we pass through the peak and minimum heat fluxes in a wall temperature-controlled experiment. In what way does a system composed of a heat source, boiling surface, and volatile liquid “see and respond to” the instability as it passes through these extrema continuously? Some insight into this question has been recently provided.

Bui and Dhir /107/ investigated transition boiling heat transfer on a vertical copper surface in a pool of saturated water. Their experiments showed that the transient q_{\max} 's were as much as 60% lower than the steady-state q_{\max} 's. Transition boiling heat transfer was very sensitive to surface condition as well as to the rate of cooling or heating of the surface. They observed two distinct transition boiling curves during transient heating and cooling. Both q_{\max} and q_{\min} could be quite different for heating as compared to cooling cases. However, the difference between the two curves diminished as the wettability of the surface increased. Bui's findings support the notion that a system might choose either or both a film-transition, or a nucleate-transition, boiling curve as it passes through the transition region.

Ramilison /108/ recently examined the behavior of boiling liquids near q_{\min} in detail. He redesigned Berenson's flat plate experiment to reduce the thermal resistance of the heating surface so that more points were accessible

in the transition regions. Experiments were made with Freon-113, acetone, benzene and n-pentane boiling on mirror-polished, roughened and teflon-coated copper surfaces. The resulting data verified certain features observed by Berenson — the modest surface finish dependence of q_{\max} , and the influence of surface chemistry on both q_{\min} and the mode of transition boiling.

Correlating the Film-transition Boiling Heat Flux. Ramiison's results led him to develop a correlative method for predicting the heat flux in the "transition-film" boiling region. He realized that, while people had previously identified the beginning of transitional boiling where the slope of the boiling curve becomes negative, we must actually identify a transition at point A in Fig. 44 — the transition at which the boiling curve starts to deviate above the non-contact film boiling curve.

It is now clear that the jump from film-transition, into nucleate-transition, boiling depends upon the magnitude of the contact angle, β . We believe that this should be the advancing angle, β_a , in film transition boiling since the heater surface must be dry before the liquid-vapor interface touches it each time. When sufficient contact occurs, the surface will cease to dry out completely between contacts, β_a will abruptly switch to the smaller value of β_r , and the mode of boiling will abruptly switch to nucleate transition boiling.

Ramiison therefore assumed that the liquid-vapor interface during film boiling takes the form of a cyclically-collapsing, two-dimensional, square array of Taylor-unstable waves as shown in Fig. 45. The size of a characteristic cell in this grid is λd .

The liquid-solid contact area can be represented as a fraction of the area of the cell, $(r/\lambda d)^2$, where r is the radius of the frustrum of the cone of liquid that contacts the surface. The duration of the contact, t_c , should be a fraction of the period of the Taylor wave which is given by equations (32) and (23/24) as

$$t_c \sim [\sigma g^3 (\rho_l - \rho_g)]^{1/4} \equiv \tau \quad (71)$$

The heat flux added to the film-boiling heat flux by transient contact, Δq , is related to the local transient heat flux resulting from liquid-solid contact. Δq is related to $q_{\text{transient}}$ by the simple energy balance,

$$\lambda_d^2(\tau)(\Delta q) \sim r^2(t_c)q_{\text{transient}} \quad (72)$$

But $q_{\text{transient}}$ is given by the semi-infinite region expression,

$$q_{\text{transient}} = \frac{k_h(T_w - T_{\text{contact}})}{(\alpha_h \tau)^{1/2}} = \frac{k_h(T_w - T_{\text{sat}})}{(\alpha_h \tau)^{1/2}} \mathcal{K} \quad (73)$$

The temperature, T_{contact} , at which contact can first occur is based on the contact of two semi-infinite regions (see e.g. /109/)

$$\frac{T_{\text{contact}} - T_{\text{sat}}}{T_w - T_{\text{sat}}} = \frac{k_l/\alpha_l^{1/2}}{k_l/\alpha_l^{1/2} + k_h/\alpha_h^{1/2}} \equiv K \quad (74)$$

where k_l , k_h , α_l , and α_h are the thermal conductivities and diffusivities of the liquid and the heater.

The limiting value of the contact temperature should then be the absolute limiting homogeneous nucleation temperature, $T_{\text{h.n.}}$, which has been shown /110/ to be well approximated by

$$T_{\text{h.n.}} = [0.923 + 0.077(T_{\text{sat}}/T_c)^9]T_c \quad (75)$$

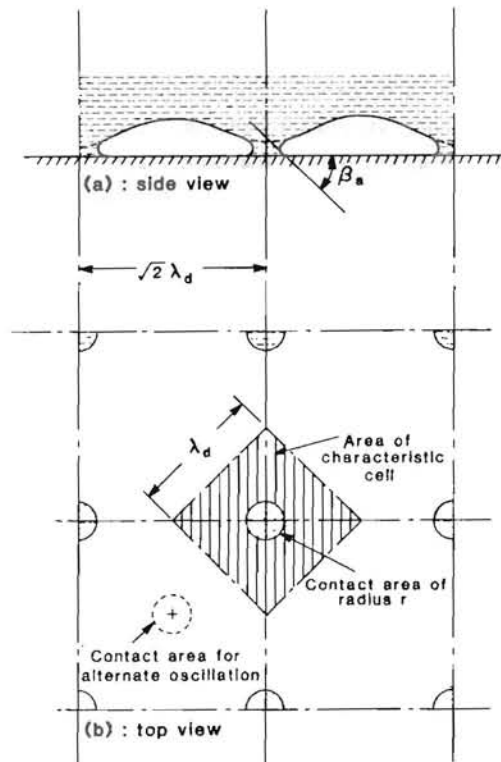


Fig. 45 The assumed pattern of transient contact during film-transition boiling on a horizontal flat plate.

Figure 46 shows the observed fraction of the limiting liquid superheat at which first liquid contact occurred in Ramilison's system. Since $(T_A - T_{sat}) / (T_{h.n.} - T_{sat})$ cannot ever exceed $K-1$ for the system, we note that as β_a approaches zero — or perfect wetting — T_A approaches the temperature required by perfect homogeneous nucleation. (Notice that $K-1$ takes up a narrow range rather than a single value owing to the slight temperature variation of the k 's and α 's.) As β_a increases, it is harder for the liquid to make contact, and easier to carry film boiling down to lower ΔT 's.

To eliminate t_c and τ Ramilison made two physical assumptions:

1. The fractional area of the contact circle increases in direct proportion to the fractional duration of contact.

$$t_c / \tau \sim (r / \lambda_d)^2 \tag{76}$$

2. Since the energy storage in the metal as a consequence of contact must be directly proportional to the additional latent heat contributed per unit cell, the fractional contact area, $(r / \lambda_d)^2$, can be proportioned as follows:

$$(r / \lambda_d)^2 \sim \frac{(\rho c_p)_h (T_A - T_w)}{\rho_g h_{fg}} \tag{77}$$

Combining equations (73), (74), (76) and (77) with (72) gave

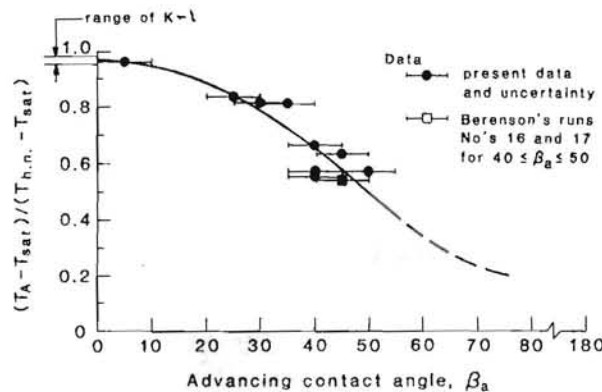


Fig. 46 Variation of the temperature of the onset of film-transition boiling with β_a .

$$\frac{\Delta q(\sigma_h \tau)^{1/2}}{\Delta T k_h} = \text{Constant} \left[\frac{(\rho c_p)_h (T_A - T_w)}{\rho_g h_{fg}} \right]^2 K \quad (78a)$$

where the groups on the left and right can be identified as modified Biot and Jakob numbers, Bi^* and Ja^* so

$$Bi^* = \text{constant}(Ja^*)^2 K \quad (78b)$$

Figure 47 compares equation (78b) with data. Notice that in this scheme of correlation, the film boiling points without contact correspond to negative Ja^* , while those in the transition-film region correspond to positive values. This comparison fixes the constant in equation (78b) as 0.374×10^{-6} .

To get Δq values Ramilison had to extrapolate the measured film boiling curve. To do this he used a modified form of Klimenko's film boiling correlation /111/ (for the turbulent, high Jakob Number case). This choice was not based on the superiority of Klimenko's model, but only on the fact that Klimenko's choice of the controlling variables in film boiling perfectly matched the measured portion of the curve. The point A was then identified as being the first point at which the film-transition boiling data deviated as much as five percent above the extrapolated curve.

Figure 47 clearly shows that film-transition boiling data of Ramilison are very well correlated by the simple equation (78b).

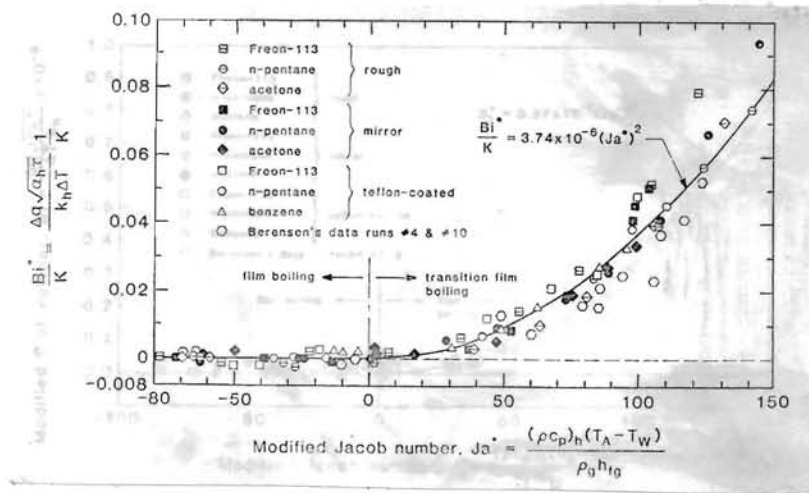


Fig. 47 Ramilison's correlation of film and film-transition boiling data for a horizontal flat plate.

Chowdhury and Winterton [112] recently measured the influence of surface roughness and β on the heat transfer from copper and aluminum cylinders quenched in water and methanol. They found that the most dramatic influence was that of the contact angle. Without exception, a decrease in contact angle caused an increase in the heat flux in the transition region. Furthermore, they say:

“The effect of contact angle extends throughout the transition boiling region, including the critical heat flux and minimum film boiling points. A lower contact angle has the effect of extending the nucleate boiling region, giving a higher critical heat flux and also it extends the transition boiling region by increasing the minimum film boiling heat flux and the associated temperature.”

This corroborates the Witte-Lienhard proposal and agrees with the recent observations of Ramlison.

These recent findings make it clear that q_{\max} and q_{\min} might not always be controlled by hydrodynamic processes alone. Wetting has a strong effect on q_{\min} (and, under some conditions, on q_{\max} as well.) The hydrodynamics of the wetting process should be investigated on a micro-level to see more clearly what happens to the conventional, hydrodynamically-controlled extrema.

It is now clear that the transition region, while it is complicated, might actually be more amenable to analysis than we had thought. It is also apparent that a true understanding of the complete boiling curve depends heavily on our understanding of behavior in the transition boiling region.

7. Summary

7.1. The State of the Hydrodynamic Theory Today

The Hydrodynamic Theory of the several boiling transitions has run its course from its rocky beginnings in the 1940's, 50's, and early 60's, through widespread acceptance in the 1970's, to what we can probably characterize as a mature skepticism in the 1980's. At this point, the following things seem fairly unassailable:

- Vapor removal during film boiling is a definite and highly predictable Taylor instability process.
- The q_{MB} and q_{\max} transitions are determined primarily by hydrodynamic instabilities.
- The transition boiling region cannot be regarded as a continuous regime.

- Transition boiling may reflect either the essential features of the potentially unstable slugs-and-columns nucleate boiling behavior, or of the cyclic Taylor collapse that marks film boiling.

However, a variety of nagging questions remain. We list some of them below. (This list is merely illustrative – not exhaustive.)

The Question as to Where the Helmholtz Instability is Located. A pernicious problem with the Zuber model for burnout is that the vapor jet behavior is hard to identify in many circumstances – in subcooled boiling, near burnout on spheres, etc. Recently Haramura and Katto /113/ suggested that the Helmholtz process is not located in the obvious jets and columns at all, but rather in the small structure of mini-jets near the surface, that feed the apparent jets from below. There is much to criticize in this theory – for example, they presume the mini-jets to collapse when their length reaches only $\lambda_H/4$. They make other assumptions that also fly in the teeth of experiments with component parts of the boiling process.

Yet the message we learn from Zuber's work – indeed from Kuhn's analysis of scientific progress, in general – is that good ideas are seldom completely correct in their original presentations. The wise investigator asks, "What can be in it?" when he looks at a new idea. It may yet be that when better experimental techniques are developed, Helmholtz processes will be found in the micro-jet structure in subcooled boiling or in certain geometries.

The Chang-Costello Question. As Bui and Dhir /107/ have recently shown, the question of non-hydrodynamic influences will not just go away, and it must be dealt with. Configurations exist in which surface effects can be greatly magnified, even though many of the influences quoted by Chang and Costello were subsequently shown to be consistent with the hydrodynamic theory. Such configurations certainly stand to lead us to a better understanding of the hydrodynamics of the q_{\max} transitions.

The q_{\min} Problem. Experiments with the onset of film-transition boiling show a clear dependence of q_{\min} on contact angle. It is also quite clear that film boiling is sure to occur when film-transition boiling becomes spinodal-limited. Is it therefore still legitimate to speak of a hydrodynamically determined q_{\min} ?

Ramilison's work /108/ suggests that q_{\min} can be determined hydrodynamically when β_a is very large. However, further work is needed to

identify that limit and to develop a correct nonlinear expression for the bubble frequency that can be used to predict it.

The Transition from Film-transition to Nucleate-transition Boiling. We have suggested that this hydrodynamic transition is dictated by a change in which a surface becomes wetted or dried so that the determining contact angle switches from β_a to β_r or vice-versa. The validity of this hypothesis needs further study, and the mechanics of such transitions need to be described in enough detail to make it possible to predict them from either side.

Flow Boiling Questions. The MESC itself — as fruitful as it has proved — needs to be looked at from the standpoint of fundamental dynamical theory. Questions have been raised as to whether or not the energy inventory statements are complete and whether or not they stand up to questions about their dependence upon coordinate selections. On a more detailed level, one would certainly hope that more absolute means might be devised to deal with the vapor blanket thickness, α , in the cylinder-in-a-crossflow problem, or the mean spray droplet diameter, δ , in the jet-disc problem.

And, of course, the MESC itself should certainly be applied to additional hydrodynamic transition questions.

The controlling mechanism for the jumps from film-transition to nucleate-transition boiling on bodies submerged in flowing liquids is still unknown. So too is the influence of forced convection on ΔT_A ; although it is known to increase q_{\min} (as well as ΔT at q_{\min}). These issues loom large in many applied process and thermohydraulic safety problems.

7.2. Some General Observations on Research in This Area

The history of the Hydrodynamic Theory reads at times like comic opera. Too often we have taken two steps backward to get three steps forward. Perhaps this is because, for a half century, we have been so driven to step forward by the terribly important problem of predicting the boiling transitions. As the need to miniaturize and intensify the processes of our technology has mounted, the intensity of the effort has risen along with it.

The processes themselves are too messy to attract the most sophisticated mathematicians and fluid mechanics of our day. Taylor and Bellman, for example, contributed much, but only in looking at clean subsets of the problem in isolation from boiling itself. Too often the study of these complex

systems is relegated to people who are pursuing short-term practical objectives. Consequently, much of the enormous output of work on the problem has consisted of isolated system-specific measurements that fail to generalize our understanding.

Yet the Hydrodynamic Theory is very rich in basic fluid mechanical and mathematical issues, and issues requiring experiments of the highest degree of sophistication. It deserves the attention of sophisticates who prefer to deal instead with a smaller set of classically-defined, and discipline-approved, problems.

Indeed the paradox of research in the field of boiling as a whole is that it is driven by such enormous practical vitality and commercial need that it has *never settled down and taken on the trappings of an academic discipline*. These trappings include:

1. Developed textbook treatments of the problem. (The nearest thing to a textbook discussion of the Hydrodynamic Theory, for example, is a single chapter in an undergraduate heat transfer book /10/.)
2. The existence of accepted authorities in the field. (It is virtually impossible to identify a true arbiter of orthodoxy and correctness in the field of boiling as a whole.)
3. Forums in which the important issues of the field can be publicly argued.

The congealing of any subject into a discipline is dangerous, of course. When it occurs, its practitioners often put on blinders and become resistant to new ideas. At the same time, the most powerful and effective *problem-solving* (a dangerous, often-misused and maligned, expression) always occurs from within a well-defined discipline.

Good science rides the razor's edge between vitality and discipline. This is a field which, while it has lacked discipline, has clearly never wanted for vitality.

"In the development of any science, the first [agreed-upon view] is usually felt to account quite successfully for most of the observations ... Further development ... calls for ... elaborate equipment, ... an esoteric vocabulary and skills, and a refinement of concepts That professionalization leads, ... to an immense restriction of the scientist's vision and to considerable resistance to ... change. The scientist has become increasingly rigid.

On the other hand, within those areas to which [the group directs

J.H. Lienhard and L.C. Witte

Reviews in Chemical Engineering

attention] normal science leads to a detail of information and to a precision of the observation-theory match that could be achieved in no other way."

Thomas S. Kuhn

8. References

1. Gouse, S.W. Jr., "An Introduction to Two-Phase Gas-Liquid Flow," Report 8734-3 Engineering Projects Lab., MIT, 1964.
2. Zuber, N., "Hydrodynamic Aspects of Boiling Heat Transfer," Ph.D. thesis, UCLA, Los Angeles, 1959. (Also available as AECU-4439 *Physics and Mathematics*.)
3. Zuber, N., Tribus, M. and Westwater, J.W., "The Hydrodynamic Crisis in the Pool Boiling of Saturated and Subcooled Liquids," *Int. Developments in Heat Transfer*, ASME, New York, 1963, pp. 230-235.
4. Leidenfrost, J.G., "On the Fixation of Water in Diverse Fire," (tr. by C. Wares from *de Aquae Communis Nonnullis Qualitatibus Tractatus*, 1756) *Int. J. Heat Mass Transfer*, Vol. 9, 1966, pp. 1153-1166.
5. Kistemaker, J., "The Spheroidal State of a Waterdrop," *Physica*, Vol. 29, 1963, pp. 96-104.
6. Kutateladze, S.S., *Teploperedacha pri Kondensatsii i Kipenii*, State Sci. and Tech. Pubs. of Lit. on Mach., Moscow, 1952. (Also published in English as *Heat Transfer in Condensation and Boiling*, 2nd ed., AEC-tr-3770, Phys. and Math. 1959.)
7. Nukiyama, S., "The Maximum and Minimum Values of the Heat Q Transmitted from Metal to Boiling Water under Atmospheric Pressure," (tr. by C.J. Lee from *J. Jap. Soc. Mech. Engr.*, Vol. 37, 1934, pp. 367-374.) *Int. J. Heat Mass Transfer*, Vol. 9, 1966, pp. 1419-1433.
8. Pilling, N.B. and Lynch, T.D., "Cooling Properties of Technical Liquids," *Trans. Am. Inst. of Mining and Met. Engrs.*, Vol. 62, 1920, pp. 665-688.
9. Drew, T.B. and Mueller, C. "Boiling," *Trans. AIChE*, Vol. 33, 1937, p. 449.
10. Lienhard, J.H., *A Heat Transfer Textbook*, Prentice Hall Inc., Englewood Cliffs, N.J., 1981.
11. Kuhn, T.H., *The Structure of Scientific Revolutions*, 2nd ed., Univ. of Chicago Press, 1970.
12. Farber, E.A. and Scoria, R.L., "Heat Transfer to Water Boiling under Pressure," *Trans. ASME*, Vol. 70, 1948, pp. 369-384.
13. Sakurai, A. and Shiotsu, M., "Temperature-controlled Pool-boiling Heat Transfer," *Proc. Fifth Int. Heat Trans. Conf.*, Vol. 4, B3.1, 1974, pp. 81-85.
14. Peterson, W.C. and Zaalouk, M.G., "Boiling-curve Measurements from a Controlled Heat-Transfer Process," *J. Heat Transfer*, Vol. 93, 1971, pp. 408-412.

15. Zhukov, S.A., and Barelko, V.V., "Nonuniform Steady State of the Boiling Process in the Transition Region Between the Nucleate and Film Regimes," *Int. J. Heat Mass Transfer*, Vol. 26, No. 8, 1983, pp. 1121-1130.
16. Pramuk, F.S. and Westwater, J.W., "Effect of Agitation on the Critical Temperature Difference for a Boiling Liquid," *Chem. Engr. Symp. Series*, Vol. 52, No. 18, 1956, pp. 79-83.
17. Berenson, P.J., "Transition Boiling from a Horizontal Surface," MIT Heat Transfer Lab. Tech. Rpt. No. 17, March 1960.
18. Hesse, G., "Heat Transfer in Nucleate Boiling, Maximum Heat Flux and Transition Boiling," *Int. J. Heat and Mass Transfer*, Vol. 16, 1973, pp. 1611-1627.
19. Bonilla, C.F. and Perry, C.W., "Heat Transmission to Boiling Binary Liquid Mixtures," *Trans. A.I.Ch.E.*, Vol. 37, 1941, pp. 269-290.
20. Cichelli, M.T. and Bonilla, C.F., "Heat Transfer to Liquids Boiling Under Pressure," *Trans. A.I.Ch.E.*, Vol. 41, 1945, p. 755.
21. Bonilla, C.F., personal communication, Aug. 21, 1979.
22. Kutateladze, S.S., "On the Transition to Film Boiling under Natural Convection," *Kotloturbostroenie*, No. 3, 1948, p. 10.
23. Chang, Y.P., "A Theoretical Analysis of Heat Transfer in Natural Convection and in Boiling," *Trans. ASME*, Vol. 79, 1957, p. 1501.
24. Lord Rayleigh, "On the Instability of Jets," *Proc. London Math. Soc.*, Vol. 10, Nov. 1878, p. 4.
25. Lord Rayleigh, *Theory of Sound*, second revised ed., Vol. II, London, 1896. (Reprinted by Dover Pubs., New York, 1945. See pp. 351-362.)
26. Bohr, N., "Determination of the Surface-Tension of Water by the Method of Jet Vibration," *Trans. Royal Soc., Series A*, Vol. 209, 1909, pp. 281-317.
27. Lamb, Sir Horace, *Hydrodynamics*, 6th ed., Cambridge Univ. Press, London, 1932. (Reprinted by Dover Pubs., New York, 1945. See pp. 472-3.)
28. Harrison, W.J., "The Influence of Viscosity on the Oscillations of Superposed Fluids," *Proc. London Math. Soc.*, Vol. 2, 1908, pp. 396-405.
29. Taylor, G.I., "The Instability of Liquid Surfaces when Accelerated in a Direction Perpendicular to their Planes. I," *Proc. Royal Soc. London, Series A*, Vol. 201, 1950, pp. 192-196.
30. Milne-Thompson, L.M. *Theoretical Hydrodynamics*, 4th ed., MacMillan Co., New York, 1960, p. 390.
31. Lewis, D.J., "The Instability of Liquid Surfaces when Accelerated in a

- Direction Perpendicular to their Planes. II," *Proc. Royal Soc., Series A*, Vol. 202, 1950, pp. 81-96.
32. Bellman, R. and Pennington, R.H., "Effects of Surface Tension and Viscosity on Taylor Instability," *Quar. Appl. Math.*, Vol. 12, 1954, p. 151-162.
 33. Haggerty, W.W. and Shea, J.F., "A Study of the Stability of Plane Fluid Sheets," *J. App. Mech.*, Vol. 22, Dec. 1955, pp. 509-514.
 34. Westwater, J.W. and Santangelo, J.G., "Photographic Study of Boiling," *Ind. Engr. Chem.*, Vol. 47, 1955, pp. 1605-10.
 35. Sernas, V., "Minimum Heat Flux in Film Boiling -- a Three Dimensional Model," *Proc. 2nd Can. Cong. Appl. Mech.*, Univ. of Waterloo, 1969, pp. 19-23.
 36. Bernath, L., "A Theory of Local Burnout and Its Application to Existing Data," *AIChE Symposium Series*, No. 30, Vol. 56, 1959, p. 59.
 37. Chang, Y-p., "Wave Theory of Heat Transfer in Film Boiling," *J. Heat Transfer*, Vol. 81, No. 1, 1959, pp. 1-12.
 38. Chang, Y-p., "Some Possible Critical Conditions in Nucleate Boiling," *J. Heat Transfer*, Vol. 85, No. 2, 1963, pp. 90-100.
 39. Costello, C.P. and Frea, W.J., "A Salient Non-Hydrodynamic Effect on Pool Boiling Burnout of Small Semi-Cylindrical Heaters," *AIChE Preprint No. 15*, 6th Nat'l. ASME/AIChE Heat Transfer Conf., Boston, Aug. 11-14, 1963.
 40. Costello, C.P. and Adams, J.M., "The Interrelation of Geometry, Orientation and Acceleration in the Peak Heat Flux Problem," *Mech. Engr. Dept. Rept.*, Univ. of Wash., Seattle (c. 1963).
 41. Westwater, J.W. and Breen, B.P., "Effect of Diameter of Horizontal Tubes of Film Boiling Heat Transfer," *Chem. Engr. Prog.*, Vol. 58, 1962, pp. 67-72.
 42. Moissis, R. and Berenson, P.J., "On the Hydrodynamic Transitions in Nucleate Boiling," *J. Heat Transfer*, Vol. 85, No. 3, 1963, pp. 221-9.
 43. Zuber, N., "Nucleate Boiling, the Region of Isolated Bubbles and the Similarity with Natural Convection," *Int. J. Heat Mass Transfer*, Vol. 6, 1963, pp. 53-78.
 44. Gaertner, R.F. and Westwater, J.W., "Population of Active Sites in Nucleate Boiling Heat Transfer," *Chem. Engr. Prog. Symp. Series*, no. 30, Vol. 56, 1960, p. 39.
 45. Bhattacharya, A. and Lienhard, J.H., "Hydrodynamic Transition in Electrolysis," *J. Basic Engr.*, Vol. 94, No. 4, 1972, pp. 804-810.

46. Nishikawa, K., Fujita, Y., Uchida, S. and Ohta, H., "Effect of Heating Surface Orientation on Nucleate Boiling Heat Transfer," *Proc. ASME-JSME Thermal Engr. Joint Conf.*, (Honolulu, Mar. 20-24, 1983) Vol. 2, ASME, New York, 1983.
47. Lienhard, J.H., "On the Two Regimes of Nucleate Boiling," *J. Heat Transfer*, Vol. 107, No. 1, 1985, pp. 262-4.
48. Lienhard, J.H. and Wong, P.T.Y., "The Dominant Unstable Wavelength and Minimum Heat Flux During Film Boiling on a Horizontal Cylinder," *J. Heat Transfer*, Vol. 86, 1964, pp. 220-6.
49. Lienhard, J.H. and Sun, K.H., "Effects of Gravity and Size Upon Film Boiling from Horizontal Cylinders," *J. Heat Transfer*, Vol. 92, No. 2, 1970, pp. 292-8.
50. Borishansky, V.M., Novikov, I.I. and Kutateladze, S.S., "Use of Thermodynamic Similarity in Generalizing Experimental Data of Heat Transfer," Paper No. 56, Int. Heat Transfer Conf., Univ. of Colo., Boulder, Aug. 1961.
51. Lienhard, J.H., "Thermodynamic and Macroscopic Aspects of Boiling," PhD Dissertation, Univ. of Calif. Inst. of Engr. Res., Berkeley, Calif., Series 163, Issue No. 3, July, 1961.
52. Lienhard, J.H. and Schrock, V.E., "The Effect of Pressure, Geometry, and the Equation of State Upon the Peak and Minimum Boiling Heat Flux," *J. Heat Transfer*, Vol. 85, No. 3, 1963, pp. 261-271.
53. Bobrovich, G.E., Gogonin, I.I., and Kutataladze, S.S., "Influence of Size of Heater Surface on the Peak Pool Boiling Heat Flux," *Jour. Appl. Mech. and Tech. Phys.*, No. 4, 1964, pp. 137-8.
54. Lienhard, J.H. and Watanabe, K., "On Correlating the Peak and Minimum Boiling Heat Fluxes with Pressure and Heater Configuration," *J. Heat Transfer*, Vol. 88, no. 1, 1966, pp. 94-100.
55. Sun, K.H. and Lienhard, J.H., "The Peak Pool Boiling Heat Flux on Horizontal Cylinders," Univ. of Ky., College of Engr., Tech. Rept. 1-68-ME-1, July 1968.
56. Sun, K.H. and Lienhard, J.H., "The Peak Pool Boiling Heat Flux on Horizontal Cylinders," *Int. J. Heat Mass Transfer*, Vol. 13, 1970, pp. 1425-1439.
57. Lienhard, J.H. and Dhir, V.K., "Hydrodynamic Prediction of Peak Pool-boiling Heat Fluxes from Finite Bodies," *J. Heat Transfer*, Vol. 95, No. 2, 1973, pp. 152-8.
58. Bakhru, N. and Lienhard, J.H., "Boiling from Small Cylinders," *Int. J. Heat Mass Transfer*, Vol. 15, 1972, pp. 2011-2025.
59. Lienhard, J.H. and Dhir, V.K., "Extended Hydrodynamic Theory of

- the Peak and Minimum Pool Boiling Heat Fluxes," NASA CR-2270, July 1973.
60. Taghavi-Tafreshi, K. and Dhir, V.K., "Taylor Instability in Boiling, Melting, and Condensation or Evaporation," *Int. J. Heat Mass Transfer*, Vol. 23, 1980, pp. 1433-1445.
 61. Lienhard, J.H., Dhir, V.K. and Rihard, D.M., "Peak Pool Boiling Heat Flux Measurements on Finite Horizontal Flat Plates," *J. Heat Transfer*, Vol. 95, 1973, pp. 477-482.
 62. Costello, C.P., Bock, C.O., and Nichols, C.C., "A Study of Induced Convection Effects in Pool Boiling Burnout," *CEP Symposium Series*, Vol. 61, 1965, pp. 271-280.
 63. Ded, J.S. and Lienhard, J.H., "The Peak Pool Boiling Heat Flux on Horizontal Cylinders," *AIChE J.*, Vol. 18, No. 2, 1972, pp. 337-342.
 64. Dhir, V.K., "Viscous Hydrodynamic Instability Theory of the Peak and Minimum Pool Boiling Heat Fluxes," Ph.D. Dissertation, Univ. of Ky., Nov. 1972. (also released as Univ. of Ky. Coll. of Engr. Rpt. No. BU100, Nov. 1972).
 65. Dhir, V.K. and Lienhard, J.H., "Taylor Stability of Viscous Fluids and Application to Film Boiling," *Int. J. Heat Mass Transfer*, Vol. 16, 1973, pp. 2097-2109.
 66. Dhir, V.K. and Lienhard, J.H., "Peak Pool Boiling Heat Flux in Viscous Liquids," *J. Heat Transfer*, Vol. 96, No. 1, 1974, pp. 71-78.
 67. Lienhard, J.H. and Keeling, K.B., Jr., "An Induced Convection Effect Upon the Peak-Boiling Heat Flux," *J. Heat Transfer*, Vol. 92, No. 1, 1970, pp. 1-5.
 68. Vliet, G.C. and Leppert, G., "Critical Heat Flux for Nearly Saturated Water Flowing Normal to a Cylinder," *J. Heat Transfer*, Vol. 86, No. 1, 1964, pp. 59-67.
 69. Leppert, G. and Pitts, C.C., "Boiling," in *Advances in Heat Transfer* (T.F. Irvine, Jr. and J.P. Hartnett, eds.), Vol. 1, Academic Press, New York, 1964.
 70. Cochran, T.H. and Andracchio, C.R., "Forced Convection Peak Heat Flux on Cylindrical Heaters in Water and Refrigerant 113," NASA D-7553, February 1974.
 71. Min, T.K., Master's Thesis, Mech. Engr. Dept., Univ. of Kentucky, Lexington, 1975.
 72. Lienhard, J.H. and Eichhorn, R., "Peak Boiling Heat Flux on Cylinders in a Crossflow," *Int. J. Heat Mass Transfer*, Vol. 19, 1976, pp. 1135-1142.
 73. Lienhard, J.H. and Hasan, M.M., "On Predicting Boiling Burnout with

- the Mechanical Energy Stability Criterion," *J. Heat Transfer*, Vol. 101, No. 2, 1979, pp. 276-9.
74. Hasan, M.Z., Hasan, M.M., Eichhorn, R. and Lienhard, J.H., "Boiling Burnout During Crossflow over Cylinders, beyond the Influence of Gravity," *J. Heat Transfer*, Vol. 103, No. 3, 1981, pp. 478-484.
 75. Kheyrandish, K.K. and Lienhard, J.H., "Mechanisms for Burnout in Saturated Flow Boiling over a Horizontal Cylinder," AICHE-ASME Nat'l. Heat Transfer Conf., Denver, Aug. 4-7, 1985.
 76. Kheyrandish, K.K. and Dalton, C., "A Flow Model for Burnout in Saturated Boiling Over a Horizontal Cylinder," AICHE-ASME Heat Transfer Conference, Denver, Aug. 4-7, 1985.
 77. Yilmaz, S. and Westwater, J.W., "Effect of Velocity on Heat Transfer to Boiling Freon-113," *J. Heat Transfer*, Vol. 101, no. 1, 1980, pp. 26-31.
 78. Broussard, R.A. and Westwater, J.W., "Boiling Heat Transfer of Freon 113 Flowing Normal to a Tube: Effect of Tube Diameter," 19th AIAA Thermophysics Conference, June 25-28, 1984, Snowmass, Colo.
 79. Katto, Y. and Monde M., "Study of Mechanism of Burnout in High Heat-Flux Boiling System with an Impinging Jet," *Proc. 5th Int. Heat Transfer Conf.*, Tokyo, Vol. 4, B6.2, 1974.
 80. Monde, M. and Katto, Y., "Burnout in High Heat-Flux Boiling System with an Impinging Jet," *Int. J. Heat Mass Transfer*, Vol. 21, 1978, pp. 295-305.
 81. Katto, Y. and Ishii, K., "Burnout in a High Heat Flux Boiling System with a Forced Supply of Liquid Through a Plane Jet," *Proc. 6th Int. Heat Transfer conf.*, Toronto, 1978.
 82. Katto, Y. and Shimizu, M., "Upper Limit of the CHF in the Forced Convection Boiling on a Heated Disc with a Small Impinging Jet," *J. Heat Transfer*, Vol. 101, No. 2, 1979, pp. 265-9.
 83. Monde, M., "Burnout Heat Flux in Saturated Forced Convection Boiling with an Impinging Jet," *Heat Transfer Japanese Research*, Vol. 9, No. 1, 1980, pp. 31-41.
 84. Lienhard, J.H. and Eichhorn, R., "On Predicting Boiling Burnout for Heaters Cooled by Liquid Jets," *Int. J. Heat and Mass Transfer*, Vol. 22, 1979, pp. 774-6.
 85. Sharan, A. and Lienhard, J.H., "On Predicting Burnout in the Jet-Disc Configuration," *J. Heat Transfer*, Vol. 107, No. 2, 1985, pp. 398-401.
 86. Nukiyama, S. and Tanasawa, Y., *Trans. Soc. Mech. Engrs. (Japan)*, Vol. 4, 1938, p. 86.

87. Witte, L.C. and Cox, J.E., "The Vapor Explosion — A Second Look," *Jour. of Metals*, Vol. 30, No. 10, Oct. 1978, pp. 29-35.
88. Morison, E.E., *Men, Machines and Modern Times*, MIT Press, Cambridge, MA, 1966, p. 154.
89. Miller, R.W., Spano, A.H., Dugone, J., Weiland, D.D. and Houghtaling, J.E., "Experimental Results and Damage Effect of Destructive Test," *Trans. Am. Nuclear Soc.*, Vol. 6, 1963, p. 138.
90. Witte, L.C. and Lienhard, J.H., "On the Existence of Two Transition Boiling Curves," *Int. J. of Heat Mass Transfer*, Vol. 25, No. 6, 1982, pp. 771-779.
91. Stevens, J.W., and Witte, L.C., "Destabilization of Vapor Film Boiling Around Spheres," *Int. J. of Heat Mass Trans.*, Vol. 16, 1973, pp. 669-678.
92. Bradfield, W.S., "Liquid-solid Contact in Stable Film Boiling," *I and E C-Fundamentals*, Vol. 5, No. 2, May, 1966, pp. 200-204.
93. Henry, R.E., "A Correlation for the Minimum Film Boiling Temperature," *AIChE Symp. Series*, No. 183, Vol. 70, 1974, pp. 81-90.
94. Henry, R.E., et al., "An Experimental Study of the Minimum Film Boiling Point for Liquid-Liquid Systems," *Proc. Fifth Int. Ht. Trans. Conf.*, Tokyo, 1974.
95. Yao, S.C. and Henry, R.E., "An Investigation of Minimum Film Boiling Temperature on Horizontal Surfaces," *J. Heat Transfer*, Vol. 100, May, 1978, pp. 260-267.
96. Ragheb, H.S., and Cheng, S.C., "Surface Wetted Area during Transition Boiling in Forced Convection Flow," *J. of Heat Transfer*, Vol. 101, No. 2, 1979, pp. 381-383.
97. Lee, L, Chen, J.C. and Nelson, R.A., "Surface Probe for Measurement of Liquid Contact in Film and Transition Boiling on High-Temperature Surfaces," *Rev. Sci. Instr.*, Vol. 53, No. 9, 1982, pp. 100-104.
98. Swanson, J.L., Bowman, H.F. and Smith, J.L., "Transient Surface Temperature Behavior in the Film Boiling Region," *Trans. CSME*, Vol. 3, 1975, pp. 131-140.
99. Groendes, V. and Mesler, R.B., "Measurement of Transient Surface Temperature Beneath Leidenfrost Water Drops," *Proc. Int. Ht. Trans. Conf.*, 1982, Munich, Paper PB 20, Vol. 4, p. 131.
100. Stephan, K., "Stabilität beim Sieden", *Brennst.-Wärme-Kraft*, Vol. 17, No. 12, 1965, pp. 571-578.
101. Stephan, K., "Übertragung hoher Wärmestromdichten in siedene Flüssigkeiten," *Chemie-Ingr. Tech.*, Vol. 38, No. 2, 1966, pp. 112-117.

102. Kovalev, S.A., "On Methods of Studying Heat Transfer in Transient Boiling," *Int. J. of Heat Mass Transfer*, Vol. 11, No. 2, 1968, pp. 279-283.
103. Grassman, P., and Zeigler, H., "Zur Stabilität von Strömungen in geschlossenen Kreisen," *Chemie-Engr. Tech.*, Vol. 41, No. 16, 1969, pp. 908-915.
104. Winterton, R.H.S., "Comment on 'On The Existence of Two "Transition" Boiling Curves'," *Int. J. of Heat Mass Transfer*, Vol. 26, 1983, pp. 1103-1104.
105. Ungar, E.K. and Eichhorn, R., "Local Surface Boiling Heat Transfer from a Quenched Sphere," *ASME Paper 82-HT-27*, New York, 1982.
106. Sankaran, S., and Witte, L.C., "Quenching of a Hollow Sphere in Methanol," *ASME HTD Vol. 47, Multiphase Flow and Heat Transfer*, New York, 1985, pp. 7-14.
107. Bui, T.D. and Dhir, V.K., "Transition Boiling on a Vertical Surface," *J. Heat Transfer*, Vol. 107, No. 4, November, 1985, pp. 756-763.
108. Ramilison, J.M., "Transition Boiling Heat Transfer and the Film-Transition Regime," Ph.D. Dissertation, Univ. of Houston, Mech. Engr. Dept., Dec. 1985.
109. Carslaw, H.S. and Jaeger, J.C., *Conduction of Heat in Solids*, 2nd ed., Oxford Univ. Press, New York, 1959.
110. Lienhard, J.H., "Corresponding States Correlations for the Spinodal and Homogeneous Nucleation Temperatures," *J. Heat Transfer*, Vol. 104, No. 2, 1982, pp. 379-381.
111. Klimenko, V.V., "Film Boiling on a Horizontal Plate - New Correlation," *Int. J. of Heat Mass Transfer*, Vol. 102, No. 1, 1970, pp. 69-79.
112. Chowdhury, S.K.R., and Winterton, R.H.S., "Surface Effects in Pool Boiling," *Int. J. of Heat Mass Transfer*, Vol. 28, No. 10, 1985, pp. 1881-1889.
113. Haramura, Y. and Katto, Y., "A New Hydrodynamic Model of Critical Heat Flux, Applicable Widely to both Pool and Forced Convection Boiling on Submerged Bodies in Saturated Liquids," *Int. J. Heat Mass Transfer*, Vol. 26, No. 3, 1983, pp. 379-399.

9. Nomenclature

- A, a empirical constants (where A might = $A(r)$)
- A_j, A_h cross-sectional area of a vapor jet, area of a heater subtended by one vapor jet
- Bi* modified Biot number defined in equations (77) and (78b).
- C unspecified constant in equation (33)
- C.V. any control volume
- c phase velocity of an interfacial disturbance, $= \omega/k$
- D disc diameter
- d diameter of the cylindrical bubble that breaks away from the vapor sheet, diameter of jet impinging on a disc
- G gravity influence parameter, defined in equation (59)
- g, g_1 gravitational acceleration, imposed acceleration parallel with g
- h depth of a fluid layer
- h_{fg} latent heat of vaporization
- I_1, I_0 0th and 1st order modified Bessel functions of the 1st kind
- Ja* Jakob number defined in equations (77) and (78b).
- K dimensionless wave number defined in equation (49), dimensionless group defined in equation (74)
- k wave number $= 2\pi/\lambda$
- Ku Kutateladze Number, defined in equation (4)
- L, L' any characteristic dimension of a system, $L/(\sigma/g(\rho_f - \rho_g))^{1/2}$
- M molecular weight, liquid viscosity parameter defined in equation (56)
- MESC Mechanical Energy Stability Criterion
- N Borishansky No. defined in equation (53)
- P parachor $= M\sigma^{1/4}(\rho_f - \rho_g)$
- p pressure
- $q, q_{max}, q_{max,Z}, q_{min}, q_{MB}$ heat flux; peak or "burnout" q , Zuber's q_{max} , minimum q in film or film-transition boiling, Moissis-Berenson transition q
- R, R_c, R_j, R' radius of a cylindrical interface, radius of a vapor blanketed cylinder, radius of a vapor jet, $R/[\sigma/g(\rho_f - \rho_g)]^{1/2}$
- $R_{x,y}, R_{tr}$ radii of curvature of an interface in the xy plane and in the transverse direction, normal to the xy plane.
- R_t, R_b any thermal resistance, the thermal resistance of the boiling process
- r radial coordinate, also ρ_f/ρ_g
- St Strouhal number, $D/u_\infty \tau$; equal to d/λ at burnout
- T, T_{sat}, T_w temperature, temperature of saturated liquid, temperature of the wall of a heater

- $T_{\text{contact}}, T_{\text{h.n.}}$ initial temperature of solid-liquid contact, homogeneous nucleation temperature
 t, t_c time, duration of liquid-solid contact
 U a fluid velocity parallel with an interface
 u, u_∞ x-direction velocity component, velocity of an incoming liquid flow
 u_g relative velocity in a vapor jet or sheet
 V vapor viscosity parameter defined in equation (52)
 v_f, v_g the "superficial" or average velocities of liquid approaching (or vapor leaving) a heater, saturated liquid and vapor volumes
 W, W_c, W' complex potential or width of Keeling's test heater, width of Keeling's test chamber, an L' based on W
 We Weber number, $2\rho_g u_\infty^2 R / \sigma$ for crossflow over a cylinder or $\rho_f u_\infty^2 D / \sigma$ for jet-disc burnout
 x, y axial and transverse coordinates
 z complex variable, $x + iy$
 α amplitude of an interfacial disturbance, ratio of vapor sheet thickness to $2R$, fraction of liquid converted to a spray in the jet-disc configuration, thermal diffusivity
 β, β_a, β_r contact angle or jet-to-disc diameter ratio, advancing β , retreating β
 Γ density parameter defined in equation (49)
 ΔT $T_w - T_{\text{sat}}$
 Δq difference between q in film-transition, and film-boiling
 δ thickness of the vapor blanket on the sides of a submerged heater near burnout, mean diameter of spray droplets
 η local displacement of an interface
 θ angle of a plate from the horizontal upward-facing position
 Λ dimensionless λ defined in equation (42)
 $\lambda, \lambda_c, \lambda_d$ wavelength, critical λ , "most dangerous" Taylor λ
 $\lambda_{H,c}, \lambda_{H,d}$ critical and "most dangerous" Helmholtz wavelength
 $\lambda_{R,c}, \lambda_{R,d}$ critical and "most dangerous" Rayleigh wavelengths
 ρ density
 σ surface tension
 τ period of bubble breakoff from sheet, characteristic time defined in equation (71)
 ϕ velocity potential, dimensionless peak heat flux, $\pi q_{\text{max}} / \rho_g h_{fg} u_\infty$ for cyl. in crossflow, $q_{\text{max}} / \rho_g h_{fg} u_\infty$ for the jet-disc burnout
 χ characteristic heat flux defined in equation (44)
 ψ stream function
 Ω dimensionless ω defined in equation (41)
 ω frequency of interfacial motion (may be real or imaginary)

General Subscripts

- A denoting separation of film-transition from film, boiling
- c denoting a thermodynamic critical T or p, or a dynamically critical λ , except as it appears in W_c , R_c , and t_c
- f,g denoting the saturated liquid and vapor states, except as they represent superficial velocities
- h denoting a property of the heater
- l denoting a liquid property
- r denoting a reduced variable — one divided by critical value

General Superscripts

- ' denoting the upper of two fluids (see Fig. 10), except as defined in an L'